$^{40}AR/^{39}AR$ DATA FROM THE TANACROSS D-1 AND PARTS OF THE D-2, C-1, AND C-2 QUADRANGLES, ALASKA

Travis J. Naibert, Jeff A. Benowitz, Alicja Wypych, Karri R. Sicard, and Evan Twelker

Raw Data File 2020-12

2020
STATE OF ALASKA
DEPARTMENT OF NATURAL RESOURCES
DIVISION OF GEOLOGICAL & GEOPHYSICAL SURVEYS

STATE OF ALASKA
Mike Dunleavy, Governor

DEPARTMENT OF NATURAL RESOURCES
Corri A. Feige, Commissioner

DIVISION OF GEOLOGICAL & GEOPHYSICAL SURVEYS
Steve Masterman, State Geologist & Director

Publications produced by the Division of Geological & Geophysical Surveys are available to download from the DGGS website (dggs.alaska.gov). Publications on hard-copy or digital media can be examined or purchased in the Fairbanks office:

Alaska Division of Geological & Geophysical Surveys (DGGS)
3354 College Road | Fairbanks, Alaska 99709-3707
Phone: 907.451.5010 | Fax 907.451.5050
dggspubs@alaska.gov | dggs.alaska.gov

DGGS publications are also available at:

Alaska State Library, Historical
Collections & Talking Book Center
395 Whittier Street
Juneau, Alaska 99801

Alaska Resource Library and
Information Services (ARLIS)
3150 C Street, Suite 100
Anchorage, Alaska 99503

Suggested citation:
Naibert, T.J., Benowitz, J.A., Wypych, Alicja, Sicard, K.R., and Twelker, Evan, 2020, 40Ar/39Ar data from the Tanacross D-1 and parts of the D-2, C-1, and C-2 quadrangles, Alaska: Alaska Division of Geological & Geophysical Surveys Raw Data File 2020-12, 35 p. http://doi.org/10.14509/30466

$^{40}AR/^{39}AR$ DATA FROM THE TANACROSS D-1 AND PARTS OF THE D-2, C-1, AND C-2 QUADRANGLES, ALASKA

Travis J. Naibert, Jeff A. Benowitz, Alicja Wypych, Karri R. Sicard, and Evan Twelker

INTRODUCTION

This report presents $^{40}Ar/^{39}Ar$ step-heating geochronology results for igneous and metamorphic rocks from the Alaska Division of Geological & Geophysical Surveys' (DGGS) geologic mapping project in the Northeast Tanacross map area in the Tanacross D-1 and parts of the D-2, C-1, and C-2 quadrangles, Alaska. Field samples were collected by the DGGS Mineral Resources section during detailed geologic mapping campaigns in 2017 and 2018.

The Northeast Tanacross map area lies within the Yukon-Tanana Upland and covers the boundary between the Fortymile River and Lake George assemblages (Dusel-Bacon and others, 2006). The map area encompasses documented porphyry Cu-Mo-Au deposits including Taurus (Harrington, 2010), Fishhook (also known as SW Pika), and Pika Canyon (U.S. Geological Survey, 2008), and is adjacent to the Fortymile Mining District (Yeend, 1996). Previously published geologic mapping includes a reconnaissance 1:250,000-scale map (Foster, 1970) and a slightly modified map published by the USGS (Wilson and others, 2015). DGGS published 1:63,360-scale geologic maps and a report for the area (Wypych and others, 2019; Wypych and others, *in press*; Naibert and others, *in press*), which contribute to the understanding of the metamorphic and igneous map units in the area, including delineating the boundary between parautochthonous North America (Lake George assemblage) and the allochthonous Yukon-Tanana terrane (Fortymile River assemblage) in multiple places. The age data in this report constrain the crystallization ages of igneous rocks and the cooling histories of metamorphic rocks in the map area and will be used to improve upon recent mapping and further refine the uplift history of eastern Interior Alaska.

DOCUMENTATION OF METHODS

Sample Collection

Fresh, unweathered samples from surface outcrops were collected by DGGS field geologists and were selected for dating based on the presence of sufficiently large crystals appropriate for dating. Sample location coordinates (in WGS84 datum) were obtained using GPS-enabled field tablets, with a typical reported accuracy of about 10 meters. Samples were examined under a binocular microscope and in thin section to select unaltered mineral phases before sample preparation.

Sample Preparation

For $^{40}Ar/^{39}Ar$ analysis, seventeen rock samples were submitted to the Geochronology Laboratory at the University of Alaska Fairbanks (UAF). The samples were crushed, sieved, washed, and hand-picked for muscovite, biotite, hornblende, and sericite mineral phases. The monitor mineral MMhb-1 (Samson and Alexander, 1987) with an age of 523.5 Ma (Renne and others, 1994) was used to monitor neutron flux (and calculate the irradiation parameter, J). The samples and standards were wrapped in aluminum foil, loaded into aluminum cans of 2.5-cm diameter and 6-cm height. The samples were irradiated in position 5c of the uranium-enriched research reactor at McMaster University in Hamilton, Ontario, Canada for 20 megawatt-hours.

Analytical Methods

Upon their return from the reactor, the samples and monitors were loaded into 2-mm-diameter holes in a copper tray, which was then loaded in an ultra-high-vacuum extraction line. The monitors were fused, and samples heated, using a 6-watt argon-ion laser following the technique described in York and others (1981), Layer and others (1987), and Benowitz and others (2014). Argon purification was achieved using a liquid nitrogen cold trap and a SAES Zr-Al getter at 400°C. The samples were analyzed in a VG-3600 mass spectrometer at the Geophysical Institute, University of Alaska Fairbanks. The argon isotopes measured were corrected for system blank and mass discrimination, as well as calcium, potassium, and chlorine interference reactions following procedures outlined in McDougall and Harrison (1999). Typical full-system 8-minute laser blank values (in moles) were generally 2×10^{-16} mol ^{40}Ar, 3×10^{-18} mol ^{39}Ar, 9×10^{-18} mol ^{38}Ar, and 2×10^{-18} mol ^{36}Ar, which are 10–50 times smaller than the sample/standard volume fractions. Correction factors for nucleogenic interferences during irradiation were determined from irradiated CaF_2 and K_2SO_4 as follows: $(^{39}Ar/^{37}Ar)Ca = 7.06 \times 10^{-4}$, $(^{36}Ar/^{37}Ar)Ca = 2.79 \times 10^{-4}$ and $(^{40}Ar/^{39}Ar)K = 0.0297$. Mass discrimination was monitored by running calibrated air shots. The mass discrimination during these experiments was 1.3 percent per mass unit. During sample analysis, calibration measurements were made on a weekly to monthly basis to check for changes in mass discrimination with no significant variation observed during these intervals.

RESULTS AND SAMPLE DESCRIPTIONS

A summary of all the $^{40}Ar/^{39}Ar$ results is provided in the accompanying data tables, with all ages quoted to the ± 1-sigma level and calculated using the constants of Renne and others (2010). The integrated age is the age given by the total gas measured and is equivalent to a potassium-argon (K-Ar) age. Age spectra, Ca/K, and Cl/K plots are included in the appendix. The spectrum provides a plateau age if three or more consecutive gas fractions represent at least 50 percent of the total gas release and are within two standard deviations of each other (Mean Square Weighted Deviation [MSWD] less than 2.5). When a spectrum did not provide a plateau age under the above definition, a weighted-average age was calculated. Below we provide additional discussion of the results of each age analysis, noting our preferred age determination.

17ET038 – Fortymile River assemblage quartzite to semischist

A homogeneous **muscovite** separate from sample 17ET038 was analyzed. A plateau age determination was not possible (3 or more consecutive steps were not within 2-sigma error), hence a weighted-average age is presented. The integrated age (152.3 ± 1.8 Ma) and the weighted-average age (149.4 ± 2.0 Ma) are within uncertainty. We prefer the weighted-average age of **149.4 ± 2.0 Ma** for sample 17ET038 as most representative of the time of argon closure for this mineral phase but acknowledge the jigsaw nature of the step-heat release pattern complicates interpretation. No isochron age determination was possible because of the homogenous radiogenic content of the release. We interpret the muscovite age to reflect metamorphic cooling of this quartzite below the closure temperature of muscovite.

Sample 17ET038 consists of 80 percent quartz, 7 percent muscovite, 7 percent biotite, 5 percent garnet, and 1 percent feldspar. Weak to moderate foliation is defined by muscovite and biotite flakes up to 0.5 mm in diameter. Minor chloritization of biotite is observed in thin section. Muscovite grains appear unaltered. Quartz grains are interlocking, subhedral, and display undulose extinction. Rare feldspars are altered to sericite. Garnet porphyroblasts up to 0.5 mm in diameter are poikiloblastic, with inclusions of quartz.

18AW068 – Lake George assemblage paragneiss

A homogeneous **muscovite** separate from sample 18AW068 was analyzed. The integrated age (111.4 ± 1.3 Ma) and the plateau age (111.2 ± 1.4 Ma) are within uncertainty. We prefer the plateau age of **111.2 ± 1.4 Ma** for sample 18AW068 as most representative of the time of argon closure for this mineral phase. No isochron age determination was possible because of the homogenous radiogenic content of the release. We interpret the muscovite age to reflect metamorphic cooling of this paragneiss below the closure temperature of muscovite.

A homogeneous **biotite** separate from sample 18AW068 was analyzed. The step-heat release age spectrum had an up-stepping age pattern where the higher-temperature steps have older ages than the lower-temperature steps, which is associated with alteration/argon loss. The integrated age (84.6 ± 1.7 Ma) and the plateau age (90.7 ± 2.0 Ma) are not within uncertainty. We prefer the plateau age of **90.7 ± 2.0 Ma** for sample 18AW068 because of the documented argon loss. No isochron age determination was possible because of the documented argon loss. We interpret the biotite age to reflect metamorphic cooling of this paragneiss below the closure temperature of biotite but acknowledge the age could have been affected by chloritization of biotite.

Sample 18AW068 consists of 43 percent quartz, 25 percent feldspar, 20 percent muscovite, 10 percent biotite, and 2 percent epidote. Strong foliation is defined by aligned biotite and muscovite. Muscovite up to 1 mm in diameter appears unaltered in thin section. Biotite, up to 0.5 mm in diameter, is partly chloritized and occurs as thinner and smaller crystals than muscovite. Quartz ranges from 0.02 to 3 mm in diameter and displays undulose extinction in thin section. Feldspars up to 1 mm long are largely sericitized, with some grains completely altered to sericite. Feldspar grains are elongate with foliation. Epidote occurs in clusters adjacent to micas within the foliation.

18ET177 – Fortymile River assemblage amphibolite

A mixed **hornblende-actinolite** separate from sample 18ET177 was analyzed. The vast majority of the gas release occurred during the last step-heat release (84 percent). A plateau age determination was not possible (less than 3 or more consecutive steps were within 2-sigma error), hence a weighted-average age is presented. The integrated age (174.1 ± 4.7 Ma) and the weighted-average age (167.1 ± 2.7 Ma) are within uncertainty. We prefer the weighted-average age of **167.1 ± 2.7 Ma** for sample 18ET177 because of the anomalous ages of the initial heating steps. No isochron age determination was possible because of the documented argon loss. The Ca/K ratio of 67/1 for the final heating step indicates the separate contains actinolite. We interpret the spectrum's age to reflect metamorphic cooling of this amphibolite below the closure temperature of hornblende but acknowledge uncertainty in the age interpretation due to the presence of actinolite in the separate.

Sample 18ET177 consists of 45 percent actinolite, 25 percent feldspar, 20 percent hornblende and 5 percent chlorite. Actinolite is colorless to pale green in thin section, is elongate, and forms a weak to moderate foliation. Hornblende crystals are generally larger than actinolite, commonly euhedral to subhedral, and appear to have grown within the foliation defined by actinolite, likely in a prograde metamorphic reaction. Feldspars occur as large aggregates of fine-grained, recrystallized feldspars with minor alteration to sericite. Chlorite appears along the edges of actinolite grains.

18ET312 – Lake George assemblage augen orthogneiss

A homogeneous **muscovite** separate from sample 18ET312 was analyzed. The integrated age (114.0 ± 1.4 Ma) and the plateau age (115.0 ± 1.5 Ma) are within uncertainty. We prefer the plateau age of 115.0 ± 1.5 Ma for sample 18ET312 because of the high atmospheric content of the lower-temperature step releases. No isochron age determination was possible because of the homogenous radiogenic content of the release. We interpret the muscovite age to reflect metamorphic cooling of this augen orthogneiss below the closure temperature of muscovite.

Sample 18ET312 consists of 40 percent quartz, 25 percent potassium feldspar, 15 percent plagioclase feldspar, 5 percent muscovite, and 5 percent tourmaline. Muscovite flakes are up to 1 mm in diameter and are unaltered. Quartz, up to 0.5 mm in diameter, is recrystallized and granoblastic. Potassium feldspar porphyroclasts form augen up to 4 mm in diameter, which often contain multiple crystals. Potassium feldspars are partially altered to quartz and sericite. Plagioclase crystals up to 0.5 mm in diameter are also sericitized along grain edges. Tourmaline crystals up to 1.5 mm in length were observed in thin section in a band parallel to foliation.

18KS062 – Lake George assemblage garnet-bearing pelitic semischist

A homogeneous **muscovite** separate from sample 18KS062 was analyzed. The integrated age (112.2 ± 1.6 Ma) and the plateau age (112.1± 1.6 Ma) are within uncertainty. We prefer the plateau age of **112.1 ± 1.6 Ma** for sample 18KS062 because of the high atmospheric content of the lower-temperature step releases. No isochron age determination was possible because of the homogenous radiogenic content of the release. We

interpret the muscovite age to reflect metamorphic cooling of this semischist below the closure temperature of muscovite.

Sample 18KS062 consists of 85 percent quartz, 8 percent muscovite, 5 percent biotite, 2 percent garnet, and 1 percent chlorite. Muscovite defines the foliation, larger grains are up to 1.5 mm in diameter, and appear unaltered. Biotite also occurs in foliation and is commonly seen surrounding garnet in thin section. Minor chlorite occurs as a retrograde mineral after biotite. Quartz is granoblastic and occurs in alternating bands of differing grain size. Grain size varies from 0.1 to 0.25 mm in diameter in finer-grained bands and up to 1 mm in diameter in coarser-grained bands. Garnet up to 1 mm in diameter is mostly equant and has sieve texture with inclusions of quartz and biotite. Garnet was also observed in clusters along foliation planes in thin section.

18KS116 – Altered granitic dike or small intrusion

A homogeneous **sericite** separate from sample 18KS116 was analyzed. The integrated age (87.1 ± 1.0 Ma) and the plateau age (87.1 ± 1.4 Ma) are within uncertainty. We prefer the plateau age of **87.1 ± 1.4 Ma** for sample 18KS116 as most representative of the time of formation for this mineral phase but acknowledge the uncertainty of the age determination given the jigsaw nature of the step-heat release pattern. No isochron age determination was possible because of the homogenous radiogenic content of the release. We interpret the sericite age to reflect post-intrusion alteration of the granite.

Sample 18KS116 consists of 45 percent quartz, 45 percent sericite, 5 percent muscovite, and 5 percent feldspar. Sericite is a very fine-grained alteration of feldspar grains. Feldspars are partially or entirely altered to sericite. Feldspar crystal shapes are euhedral and up to 1 mm in length. Quartz is subhedral to euhedral, equant, and ranges in size from 0.05 to 1 mm in diameter. Muscovite grains up to 0.5 mm in diameter are interpreted as primary, have no preferred orientation, and appear unaltered since crystallization.

18KS131 – Lake George assemblage quartz schist

A homogeneous **muscovite** separate from sample 18KS131 was analyzed. The integrated age (115.4 ± 2.9 Ma) and the plateau age (114.2 ± 2.7 Ma) are within uncertainty. We prefer the plateau age of **114.2 ± 2.7 Ma** for sample 18KS131 because of the high atmospheric content of the lower-temperature step releases. No isochron age determination was possible because of the homogenous radiogenic content of the release. We interpret the muscovite age to reflect metamorphic cooling of this schist below the closure temperature of muscovite.

A homogeneous **biotite** separate from sample 18KS131 was analyzed. The step-heat release age spectrum had a slight up-stepping age pattern where the higher temperature steps have older ages than the lower temperature steps, which is associated with alteration/argon loss. A plateau age determination was not possible (less than 50 percent of the ^{39}Ar release, less than 3 or more consecutive steps within 2-sigma error), hence a weighted-average age is presented. The integrated age (103.6 ± 1.3 Ma) and the weighted average age (106.4 ± 0.3 Ma) are not within uncertainty. We prefer the weighted-average age of **106.4 ± 0.3 Ma** for sample 18KS131 because of the documented argon loss. No isochron age determination was possible because of the documented argon loss. We interpret the biotite age to reflect metamorphic cooling of this schist below the closure temperature of biotite.

Sample 18KS131 consists of 40 percent quartz, 30 percent feldspar, 15 percent biotite, 10 percent muscovite, and 5 percent garnet. Alternating bands of just biotite and of biotite, muscovite, and garnet form the foliation. Biotite grain size is generally less than 1 mm in diameter. The biotite is strongly pleochroic from light tan to medium brown in thin section. Muscovite grains are generally larger than biotite, up to 3 mm in diameter, and rarely occur as mica fish. Garnets are up to 1 mm in diameter, are subhedral, and are commonly associated with muscovite foliation bands. Garnets contain few mica inclusions. Quartz is subhedral to anhedral, subequant, and commonly less than 0.2 mm in diameter. Few quartz grains are up to 1 mm in diameter. Feldspars are subhedral to anhedral and up to 1mm long. Crystals often display polysynthetic twinning, especially adjacent to biotite foliation bands.

18KS133 – Lake George assemblage orthogneiss

A homogeneous **muscovite** separate from sample 18KS133 was analyzed. The integrated age (110.9 ± 1.8 Ma) and the plateau age (111.2 ± 1.7 Ma) are within uncertainty. We prefer the plateau age of **111.2 ± 1.7 Ma** for sample 18KS133 because of the high atmospheric content of the lower-temperature step release. No isochron age determination was possible because of the homogenous radiogenic content of the release. We interpret the muscovite age to reflect metamorphic cooling of this orthogneiss below the closure temperature of muscovite.

Sample 18KS133 consists of 40 percent feldspar, 40 percent quartz, 15 percent muscovite, and 5 percent biotite. Muscovite forms the foliation along with chloritized biotite. Muscovite grains are up to 1.5 mm in diameter and are generally larger than biotite, which are less than 0.5 mm in diameter. Biotite is partially altered to chlorite. Quartz is subhedral to euhedral, up to 1 mm in diameter and down to very fine grain sizes. Larger quartz grains are rarely elongate along foliation. Feldspar grains are up to 1 mm long, commonly subhedral, and are weakly altered to sericite.

18KS199 – Lake George assemblage augen orthogneiss

A homogeneous **muscovite** separate from sample 18KS199 was analyzed. The integrated age (118.4 ± 3.2 Ma) and the plateau age (115.8 ± 3.0 Ma) are within uncertainty. We prefer the plateau age of **115.8 ± 3.0 Ma** for sample 18KS199 because of the high atmospheric content of the lower-temperature step releases. No isochron age determination was possible because of the homogenous radiogenic content of the release. We interpret the muscovite age to reflect metamorphic cooling of this orthogneiss below the closure temperature of muscovite.

A homogeneous **biotite** separate from sample 18KS199 was analyzed. The step-heat release age spectrum had a slight up-stepping age pattern where the higher-temperature steps have older ages than the lower-temperature steps, which is associated with alteration/argon loss. The integrated age (107.3 ± 1.3 Ma) and the plateau age (109.3 ± 1.3 Ma) are within uncertainty. We prefer the plateau age of **109.3 ± 1.3 Ma** for sample 18KS199 because of the documented argon loss. No isochron age determination was possible because of the documented argon loss. We interpret the biotite age to reflect metamorphic cooling of this orthogneiss below the closure temperature of biotite.

Sample 18KS199 consists of 45 percent feldspar, 35 percent quartz, 15 percent muscovite, 5 percent biotite, and 1 percent magnetite. Muscovite and biotite define the foliation. Muscovite grains are up to 1 mm in diameter and rarely form round masses within the foliation. Biotite grains are typically smaller than muscovite, with the largest grains up to 0.8 mm in diameter. Quartz grains range in size from 0.05 to 1.2 mm in diameter and often form aggregates up to 8 mm across with abundant magnetite inclusions. Feldspars up to 0.5 mm long are often weakly altered to sericite.

18KS208 – Lake George assemblage augen orthogneiss

A homogeneous **muscovite** separate from sample 18KS208 was analyzed. The step-heat-release age spectrum has a slight up-stepping age pattern where the higher-temperature steps have older ages than the lower-temperature steps, which is associated with alteration/argon loss. The integrated age (114.3 ± 1.4 Ma) and the plateau age (115.2 ± 2.0 Ma) are within uncertainty. We prefer the plateau age of **115.2 ± 2.0 Ma** for sample 18KS208 because of the documented argon loss. No isochron age determination was possible because of the documented argon loss. We interpret the muscovite age to reflect metamorphic cooling of this orthogneiss below the closure temperature of muscovite.

A homogeneous **biotite** separate from sample 18KS208 was analyzed. The step-heat-release age spectrum has an up-stepping age pattern where the higher-temperature steps have older ages than the lower-temperature steps, which is associated with alteration/argon loss. A plateau age determination was not possible (less than 50 percent of the ^{39}Ar release), hence a weighted-average age is presented. The integrated age (106.7 ± 1.3 Ma) and the weighted-average age (106.6 ± 1.4 Ma) are within uncertainty. We prefer the weighted-average age of **106.6 ± 1.4 Ma** for sample 18KS208 because of the documented argon loss. No isochron age determination was possible because of the documented argon loss. We interpret the biotite age to reflect metamorphic cooling of this orthogneiss below the closure temperature of biotite.

Sample 18KS208 consists of 35 percent quartz, 27 percent plagioclase feldspar, 20 percent potassium feldspar, 5 percent muscovite, and 3 percent biotite. Quartz crystals are up to 0.5 mm in diameter. Plagioclase grains up to 0.25 mm long are partially sericitized. Potassium feldspar grains are up to 2 mm long, are often twinned and are commonly sericitized. Muscovite and biotite up to 0.5 mm in diameter appear unaltered in thin section.

18MBW399 – Fortymile River assemblage paragneiss

A homogeneous **muscovite** separate from sample 18MBW399 was analyzed. The integrated age (163.1 ± 2.0 Ma) and the plateau age (163.9 ± 2.7 Ma) are within uncertainty. We prefer the plateau age of **163.9 ± 2.7 Ma** for sample 18MBW399 because of the high atmospheric content of the lower-temperature step releases. No isochron age determination was possible because of the homogenous radiogenic content of the release. We interpret the muscovite age to reflect metamorphic cooling of this paragneiss below the closure temperature of muscovite.

Sample 18MBW399 consists of 50 percent quartz, 20 percent muscovite, 15 percent biotite, 14 percent feldspar, and 1 percent garnet. Muscovite up to 0.5 mm in diameter appears unaltered. Biotite, up to 0.5 mm in diameter, is strongly chloritized. Feldspars are strongly sericitized. Garnets have sieve texture with quartz,

chlorite, and biotite as inclusions and around grain edges. Quartz grains vary in size from 0.01 to 0.5 mm in diameter.

18MLW126 – Lake George assemblage augen orthogneiss

A homogeneous **muscovite** separate from sample 18MLW126 was analyzed. The integrated age (121.1 ± 1.5 Ma) and the plateau age (120.9 ± 1.4 Ma) are within uncertainty. We prefer the plateau age of **120.9 ± 1.4 Ma** for sample 18MLW126 because of the high atmospheric content of the lower-temperature step release. No isochron age determination was possible because of the homogenous radiogenic content of the release. We interpret the muscovite age to reflect metamorphic cooling of this orthogneiss below the closure temperature of muscovite.

A homogeneous **biotite** separate from sample 18MLW126 was analyzed. The step-heat-release age spectrum has a slight up-stepping age pattern where the higher-temperature steps have older ages than the lower-temperature steps, which is associated with alteration/argon loss. The integrated age (109.3 ± 1.4 Ma) and the plateau age (110.4 ± 2.1 Ma) are within uncertainty. We prefer the plateau age of **110.4 ± 2.1 Ma** for sample 18MLW126 because of the documented argon loss. No isochron age determination was possible because of the documented argon loss. We interpret the biotite age to reflect metamorphic cooling of this orthogneiss below the closure temperature of biotite.

Sample 18MLW126 consists of 43 percent quartz, 20 percent plagioclase feldspar, 30 percent potassium feldspar, 5 percent muscovite, 2 percent biotite, and trace zircon. Quartz ranges in size up to 1mm in diameter, is recrystallized with long axes in the direction of strain, and has undulose extinction in thin section. Small inclusions of opaque minerals and zircon are present in quartz grains. Plagioclase up to 1 mm long are anhedral and partially sericitized. Anhedral potassium feldspars are also up to 1mm long, and surround larger, subhedral potassium feldspar augen up to 6 mm long. Muscovite up to 1 mm in diameter and biotite up to 0.5 mm in diameter are fragmented and define the foliation. Some of the biotite is chloritized.

18MLW132 – Fortymile River assemblage garnet-bearing paragneiss

A homogeneous **biotite** separate from sample 18MLW132 was analyzed. The step-heat-release age spectrum has an up-stepping age pattern where the higher-temperature steps have older ages than the lower-temperature steps, which is associated with alteration/argon loss. A plateau age determination was not possible (less than 50 percent of the ^{39}Ar release), hence a weighted-average age is presented. The integrated age (123.9 ± 1.8 Ma) and the weighted-average age (122.4 ± 2.1 Ma) are within uncertainty. We prefer the weighted-average age of **122.4 ± 2.1 Ma** for sample 18MLW132 because of the documented argon loss. No isochron age determination was possible because of the documented argon loss. We interpret the biotite age to reflect metamorphic cooling of this paragneiss below the closure temperature of biotite.

Sample 18MLW132 consists of 35 percent sericite, 30 percent quartz, 20 percent biotite, 8 percent garnet, 5 percent opaque minerals, and 2 percent muscovite. Sericite is a fine-grained alteration of feldspar and mica grains. Quartz up to 1 mm in diameter displays undulose extinction in thin section. Biotite in foliation planes with quartz and altered feldspar appears to be primary biotite. Biotite and chlorite around garnet porphyroblasts appear to be secondary, retrograde minerals. Most biotite is partially chloritized. Garnet

porphyroblasts are up to 2 mm in diameter. Opaque minerals in thin section occur along foliation and commonly within biotite and chlorite. Minor muscovite up to 0.5 mm in diameter also occur along foliation.

18RN122 – Fortymile River assemblage orthogneiss

A homogeneous **muscovite** separate from sample 18RN122 was analyzed. The integrated age (159.9 ± 2.2 Ma) and the plateau age (161.3 ± 2.9 Ma) are within uncertainty. We prefer the plateau age of **161.3 ± 2.9 Ma** for sample 18RN122 because of the high atmospheric content of the lower-temperature step releases. No isochron age determination was possible because of the homogenous radiogenic content of the release. We interpret the muscovite age to reflect metamorphic cooling of this orthogneiss below the closure temperature of muscovite.

Sample 18RN122 consists of 45 percent quartz, 30 percent plagioclase feldspar, 10 percent potassium feldspar, and 15 percent muscovite. Quartz varies in size from 0.1 to 2 mm in diameter. Undulose extinction was observed in thin section and quartz is often recrystallized in aggregates of grains in the direction of strain. Plagioclase feldspars are anhedral, average 0.5 mm long, and are up to 1 mm long. Potassium feldspars are generally no larger than 0.5 mm long. Feldspars are partially altered to sericite. Muscovite up to 1 mm in diameter define the foliation.

18RN259 – Fortymile River assemblage graphitic quartz schist

A homogeneous **muscovite** separate from sample 18RN259 was analyzed. The integrated age (121.6 ± 2.0 Ma) and the plateau age (120.7 ± 2.0 Ma) are within uncertainty. We prefer the plateau age of **120.7 ± 2.0 Ma** for sample 18RN259 because of the high atmospheric content of the lower-temperature step releases. No isochron age determination was possible because of the homogenous radiogenic content of the release. We interpret the muscovite age to reflect metamorphic cooling of this schist below the closure temperature of muscovite.

A homogeneous **biotite** separate from sample 18RN259 was analyzed. The step-heat-release age spectrum has a slight up-stepping age pattern where the higher-temperature steps have older ages than the lower-temperature steps, which is associated with alteration/argon loss. A plateau age determination was not possible (less than 50 percent of the ^{39}Ar release), hence a weighted-average age is presented. The integrated age (118.5 ± 1.7 Ma) and the weighted-average age (108.2 ± 3.0 Ma) are not within uncertainty. We prefer the weighted-average age of **108.2 ± 3.0 Ma** for sample 18RN259 because of the documented argon loss. No isochron age determination was possible because of the documented argon loss. We interpret the biotite age to reflect metamorphic cooling of this schist below the closure temperature of biotite.

Sample 18RN259 consists of 60 percent quartz, 15 percent muscovite, 15 percent biotite, 5 percent garnet, 4 percent feldspar, 1 percent graphite, and trace zircon. Quartz grains range from 0.01 to 0.5 mm in diameter and are anhedral and recrystallized. Muscovite and biotite up to 1 mm in diameter define the foliation along with minor graphite. Garnet porphyroblasts up to 0.5 mm in diameter are often resorbed and fragmented. Garnet porphyroblasts have strain shadows containing quartz and biotite, as well as numerous quartz inclusions. Feldspar is partially altered to sericite.

18RN358 – Fortymile River assemblage paragneiss

A homogeneous **muscovite** separate from sample 18RN358 was analyzed. The integrated age (154.2 ± 1.8 Ma) and the plateau age (152.5 ± 1.9 Ma) are within uncertainty. We prefer the plateau age of **152.5 ± 1.9 Ma** for sample 18RN358 as most representative of the time of argon closure for this mineral phase but acknowledge the jigsaw nature of the step-heat release pattern complicates interpretation. No isochron age determination was possible because of the homogenous radiogenic content of the release. We interpret the muscovite age to reflect metamorphic cooling of this paragneiss below the closure temperature of muscovite.

A homogeneous **biotite** separate from sample 18RN358 was analyzed. The step-heat-release age spectrum has a hump-shaped age pattern where the middle-temperature steps have older ages than the lower- and higher-temperature steps. Younger lower-temperature steps are likely associated with alteration/argon loss. The integrated age (88.9 ± 1.4 Ma) and the plateau age (96.4 ± 2.3 Ma) are within uncertainty. We prefer the plateau age of **96.4 ± 2.3 Ma** for sample 18RN358 because of the documented argon loss. No isochron age determination was possible because of the documented argon loss. We interpret the biotite age to reflect alteration or reheating of biotite, possibly due to fluids or nearby magmatism.

Sample 18RN358 consists of 60 percent quartz, 25 percent muscovite, 10 percent biotite, 5 percent garnet. Quartz grains vary in size up to 2 mm in diameter and clusters of granoblastic quartz grains are elongated with foliation. Muscovite up to 1 mm in diameter defines the foliation. Biotite is smaller than muscovite, appears in the foliation with muscovite, and also occurs around garnet edges. Garnet up to 1 mm in diameter is partially resorbed and surrounded by biotite.

18TJN068 – Lake George assemblage augen orthogneiss

A homogeneous **muscovite** separate from sample 18TJN068 was analyzed. The integrated age (109.5 ± 2.0 Ma) and the plateau age (109.5 ± 1.8 Ma) are within uncertainty. We prefer the plateau age of **109.5 ± 1.8 Ma** for sample 18TJN068 because of the high atmospheric content of the lower-temperature step releases. No isochron age determination was possible because of the homogenous radiogenic content of the release. We interpret the muscovite age to reflect metamorphic cooling of this orthogneiss below the closure temperature of muscovite.

A homogeneous **biotite** separate from sample 18TJN068 was analyzed. The step-heat-release age spectrum has a slight up-stepping age pattern where the higher-temperature steps have older ages than the lower-temperature steps, which is associated with alteration/argon loss. The integrated age (106.3 ± 1.4 Ma) and the plateau age (110.2 ± 2.1 Ma) are not within uncertainty. We prefer the plateau age of **110.2 ± 2.1 Ma** for sample 18TJN068 because of the documented argon loss. No isochron age determination was possible because of the documented argon loss. We interpret the biotite age to reflect metamorphic cooling of this orthogneiss below the closure temperature of biotite.

Sample 18TJN068 consists of 40 percent quartz, 20 percent potassium feldspar, 20 percent plagioclase, 10 percent biotite, and 10 percent muscovite. Granoblastic quartz is up to 1 mm in diameter. Potassium feldspar porphyroclasts are up to 8 mm long. Plagioclase grains are up to 0.5 mm long. Many feldspar grains

are partially sericitized. Biotite up to 0.25 mm in diameter is partially chloritized. Muscovite up to 0.5 mm in diameter defines the foliation along with biotite.

ACKNOWLEDGMENTS

The DGGS Northeast Tanacross project was funded through State of Alaska general funds and by the USGS National Cooperative Geologic Mapping Program under STATEMAP award number G18AC00137 for 2018. The authors acknowledge the contributions of the 2017 and 2018 Northeast Tanacross project field crew: Melanie B. Werdon, Jen E. Athey, Amanda L. Willingham, Alec C. Lockett, Rainer J. Newberry, and W. Chris Wyatt.

REFERENCES

Benowitz, J.A., Layer, P.W., and VanLaningham, Sam, 2014, Persistent long-term (~24 Ma) exhumation in the eastern Alaska Range constrained by stacked thermochronology: Geological Society of London Special Publication 378, p. 225–243.

Dusel-Bacon, Cynthia., Hopkins, M.J., Mortensen, J.K., Dashevsky, S.S., Bressler, J.R., and Day, W.C., 2006, Paleozoic tectonic and metallogenic evolution of the pericratonic rocks of east-central Alaska and adjacent Yukon, *in* Colpron, Maurice, and Nelson, J.L. eds., Paleozoic Evolution and Metallogeny of Pericratonic Terranes at the Ancient Pacific Margin of North America, Canadian and Alaskan Cordillera: Geological Association of Canada Special Paper 45, p. 25–74.

Foster, H.L., 1970, Reconnaissance Geologic Map of the Tanacross Quadrangle, Alaska: U.S. Geological Survey Miscellaneous Geologic Investigations Map 593, 1 sheet, scale 1:250,000.

Harrington, Edward, 2010, Taurus Property: Technical Report for Senator Minerals Inc., 133 p. (posted on www.sedar.com).

Layer, P.W., Hall, C.M. and York, Derek, 1987, The derivation of $^{40}Ar/^{39}Ar$ age spectra of single grains of hornblende and biotite by laser step heating: Geophysical Research Letters, v. 14, p. 757–760.

McDougall, Ian and Harrison, T.M., 1999, Geochronology and Thermochronology by the $^{40}Ar/^{39}Ar$ method, 2nd edition, Oxford University Press, New York, 269 p.

Naibert, T.J., Benowitz, J.A., Wypych, Alicja, Sicard, K.R., and Twelker, Evan, *in press*, Metamorphic cooling history of the Fortymile and Lake George assemblages from $^{40}Ar/^{39}Ar$ data from the northeast Tanacross Quadrangle, Alaska: Alaska Division of Geological & Geophysical Surveys Report of Investigation RI 2020-9F.

Renne, P.R., Deino, A.L., Walter, R.C., Turrin, B.D., Swisher, C.C., Becker, T.A., Curtis, G.H., Sharp. W.D., and Jaouni, A.R., 1994, Intercalibration of astronomical and radioisotopic time: Geology, v. 22, n. 9, p. 783–786.

Renne, P.R., Mundil, Roland, Balco, Greg, Min, Kyoungwon, and Ludwig, K.R., 2010, Joint determination of ^{40}K decay constants and $^{40}Ar^*/^{40}K$ for the Fish Canyon sanidine standard, and improved accuracy for $^{40}Ar/^{39}Ar$ geochronology: Geochimica et Cosmochimica Acta, v. 74, n. 18, p. 5,349–5,367.

Samson, S.D., and Alexander, E.C., 1987, Calibration of the interlaboratory $^{40}Ar/^{39}Ar$ dating standard, MMhb1: Chemical Geology, v. 66, p. 27–34.

U.S. Geological Survey, 2008, Alaska resource data file, new and revised records version 1.7: U. S. Geological Survey Open-File Report 2008-1225, p. 2,144–2,149.

Wilson, F.H., Hults, C.P., Mull, C.G., and Karl, S.M., 2015, Geologic map of Alaska: U.S. Geological Survey Scientific Investigations Map 3340, 197 p., 2 sheets, scale 1:1,584,000.

Wypych, Alicja, Hubbard, T.D., Naibert, T.J., Athey, J.E., Newberry, R.J., Sicard, K.R., Twelker, Evan, Werdon, M.B., Willingham, A.L., Wyatt, W.C., and Lockett, A.C., 2019, Northeastern Tanacross geologic map, Tanacross D-1, D-2, C-1, and C-2 quadrangles, Alaska: Alaska Division of Geological & Geophysical Surveys Preliminary Interpretive Report 2019-6, 20 p., 1 sheet, scale 1:63,360. http://doi.org/10.14509/30197

Wypych, Alicja, Hubbard, T.D., Naibert, T.J., Athey, J.E., Newberry, R.J., Sicard, K.R., Twelker, Evan, Werdon, M.B., Willingham, A.L., Wyatt, W.C., and Lockett, A.C., *in press*, Northeastern Tanacross geologic map, Tanacross D-1, D-2, C-1, and C-2 quadrangles, Alaska: Alaska Division of Geological & Geophysical Surveys Report of Investigation 2020-9, 1 sheet, scale 1:63,360.

Yeend, Warren, 1996, Gold placers of the historical Fortymile River region, Alaska: U.S. Geological Survey Bulletin 2125, 75 p., 1 sheet, scale 1:63,360.

York, Derek., Hall, C.M., Yanase, Yotaro, Hanes, J.A., and Kenyon, W.J., 1981, $^{40}Ar/^{39}Ar$ dating of terrestrial minerals with a continuous laser: Geophysical Research Letters, v. 8, p. 1136–1138.

APPENDIX: PLOTS OF $^{40}AR/^{39}AR$ AGE SPECTRA AND CA/K AND CL/K RATIOS

Steps filled in gray were used for plateau and weighted-average age determinations.

17ET038

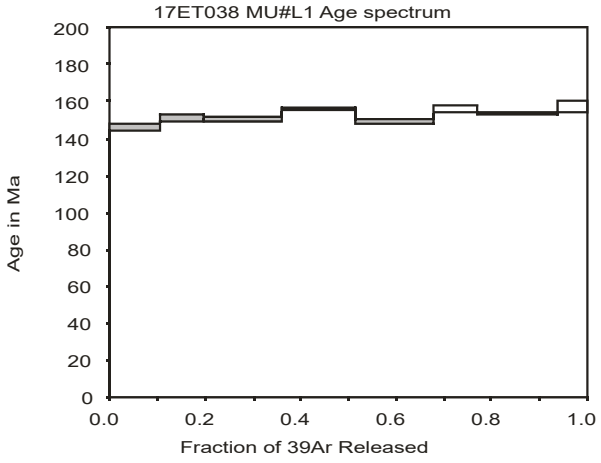

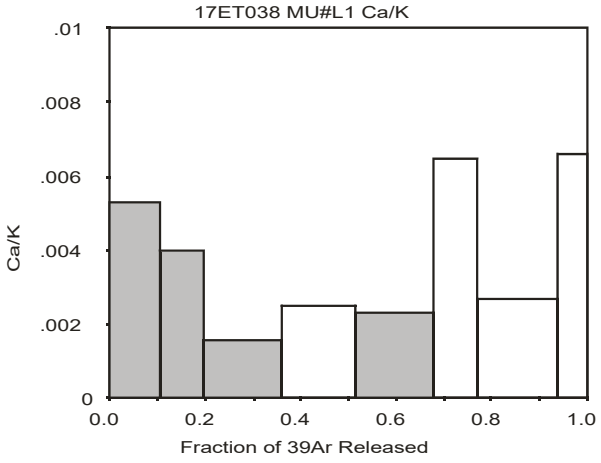

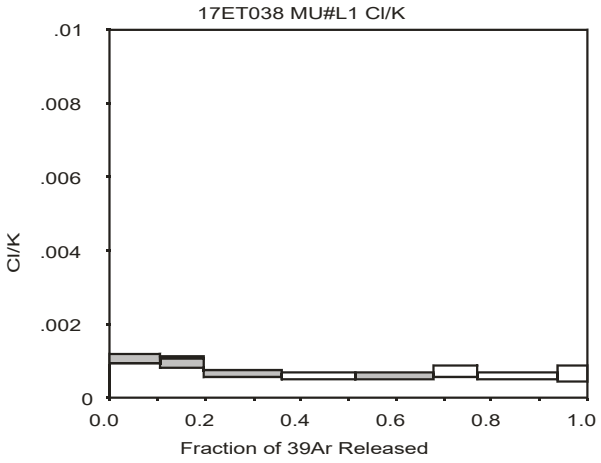

18AW068

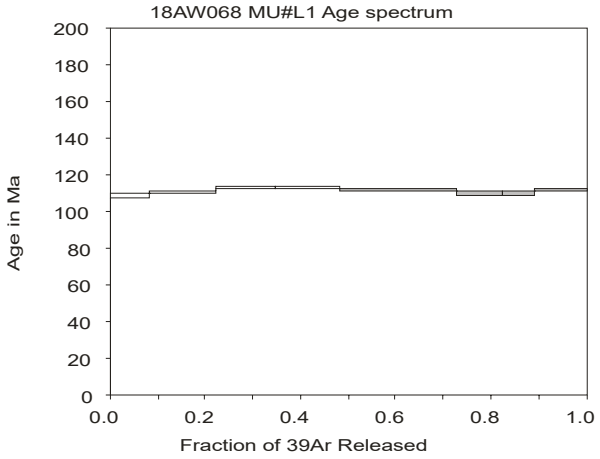
18AW068 MU#L1 Age spectrum
Age in Ma
Fraction of 39Ar Released

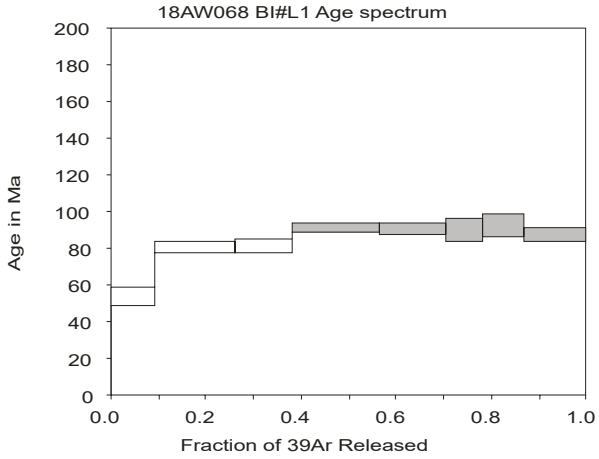
18AW068 BI#L1 Age spectrum
Age in Ma
Fraction of 39Ar Released

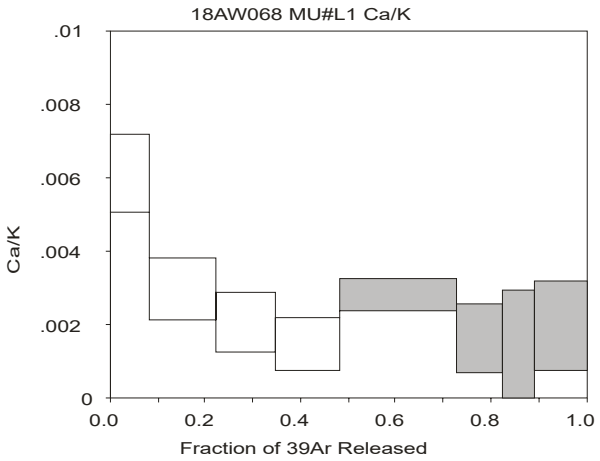
18AW068 MU#L1 Ca/K
Ca/K
Fraction of 39Ar Released

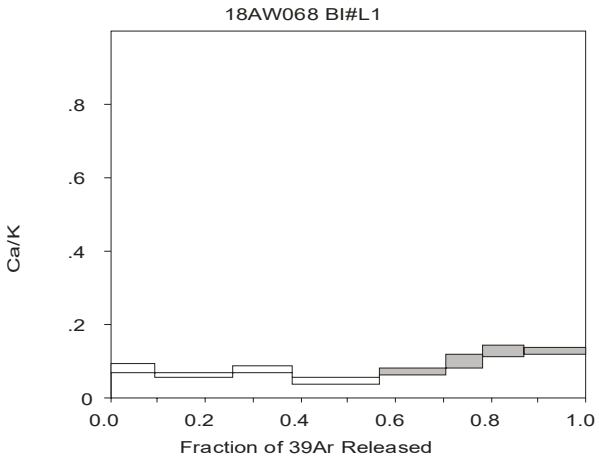
18AW068 BI#L1
Ca/K
Fraction of 39Ar Released

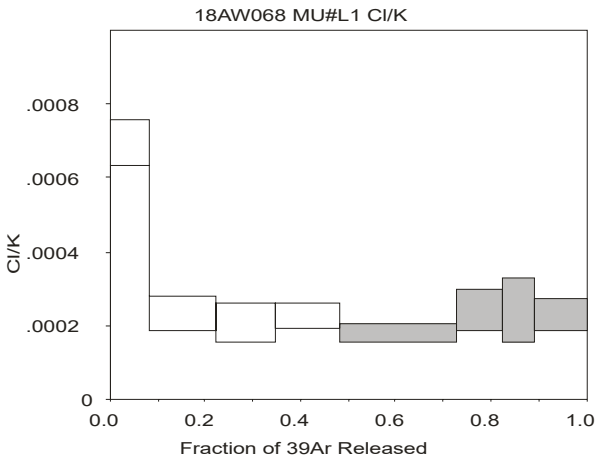
18AW068 MU#L1 Cl/K
Cl/K
Fraction of 39Ar Released

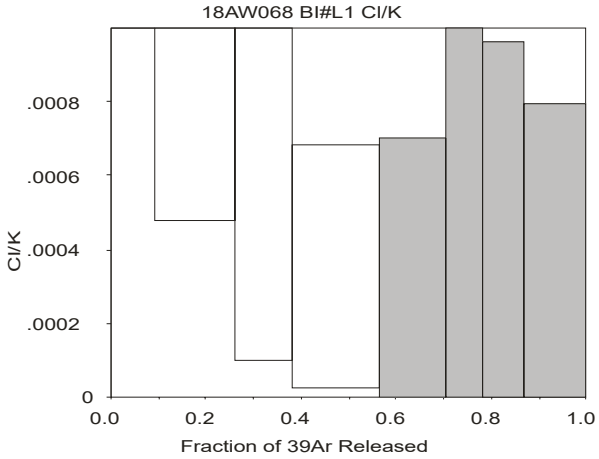
18AW068 BI#L1 Cl/K
Cl/K
Fraction of 39Ar Released

18ET177

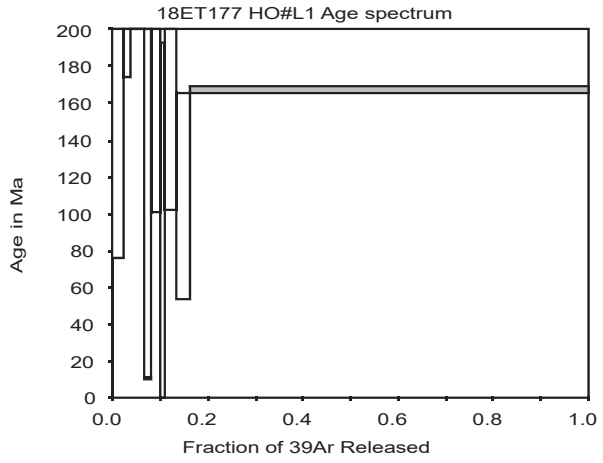
18ET177 HO#L1 Age spectrum
Age in Ma
200
180
160
140
120
100
80
60
40
20
0
0.0
0.2
0.4
0.6
0.8
1.0
Fraction of 39Ar Released

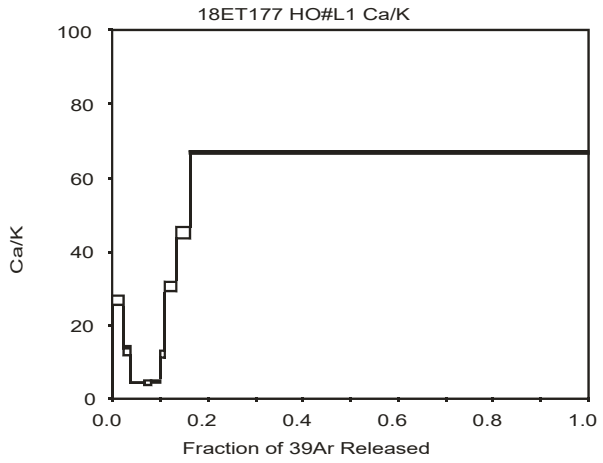
18ET177 HO#L1 Ca/K
Ca/K
100
80
60
40
20
0
0.0
0.2
0.4
0.6
0.8
1.0
Fraction of 39Ar Released

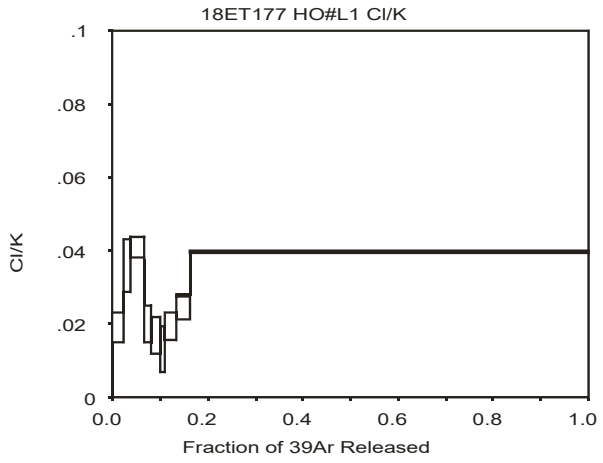
18ET177 HO#L1 Cl/K
Cl/K
.1
.08
.06
.04
.02
0
0.0
0.2
0.4
0.6
0.8
1.0
Fraction of 39Ar Released

18ET312

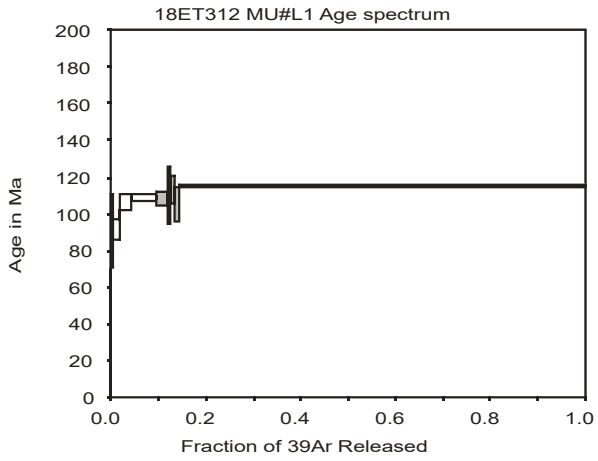
18ET312 MU#L1 Age spectrum
Age in Ma
200
180
160
140
120
100
80
60
40
20
0
0.0
0.2
0.4
0.6
0.8
1.0
Fraction of 39Ar Released

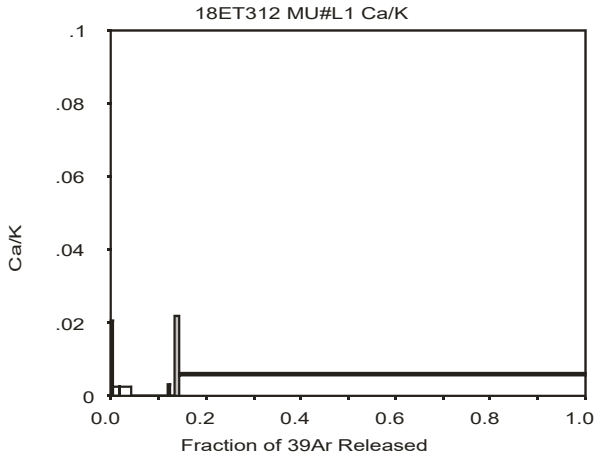
18ET312 MU#L1 Ca/K
Ca/K
.1
.08
.06
.04
.02
0
0.0
0.2
0.4
0.6
0.8
1.0
Fraction of 39Ar Released

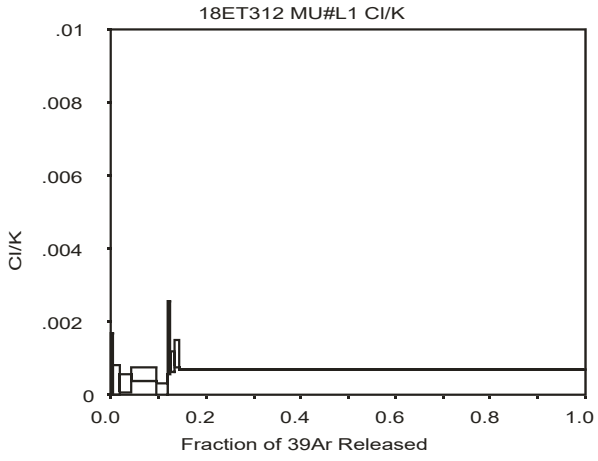
18ET312 MU#L1 Cl/K
Cl/K
.01
.008
.006
.004
.002
0
0.0
0.2
0.4
0.6
0.8
1.0
Fraction of 39Ar Released

18KS062

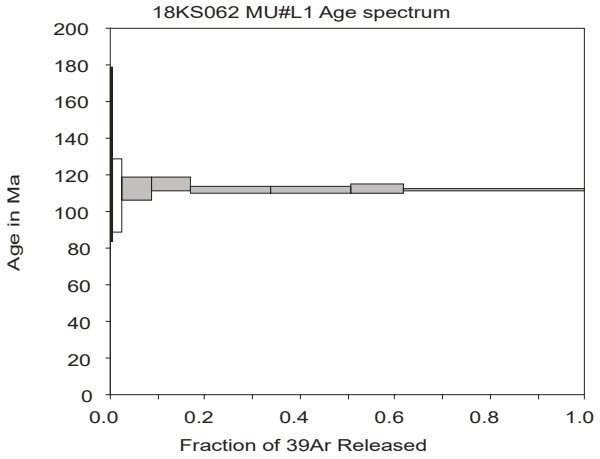
18KS062 MU#L1 Age spectrum
Age in Ma
200
180
160
140
120
100
80
60
40
20
0
0.0
0.2
0.4
0.6
0.8
1.0
Fraction of 39Ar Released

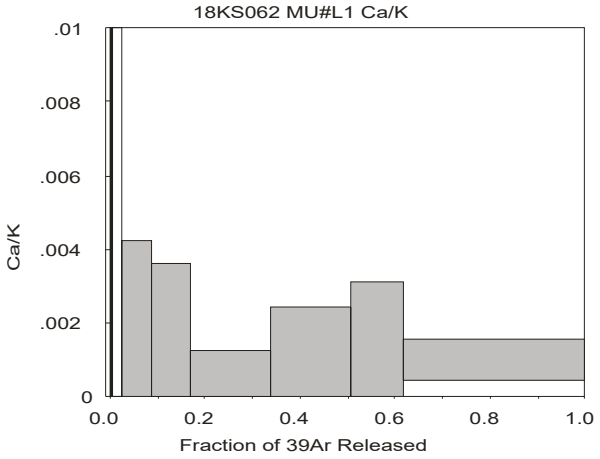
18KS062 MU#L1 Ca/K
Ca/K
.01
.008
.006
.004
.002
0
0.0
0.2
0.4
0.6
0.8
1.0
Fraction of 39Ar Released

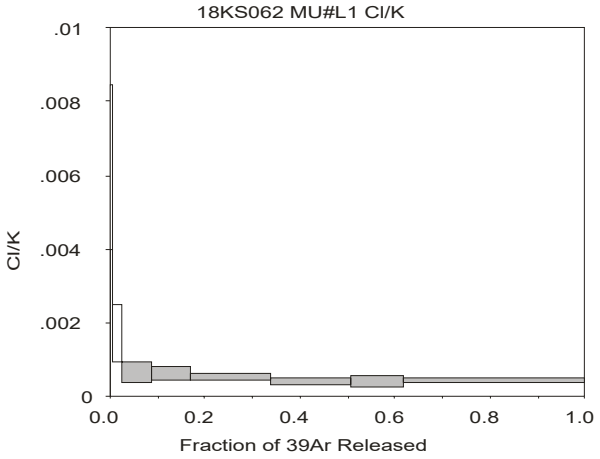
18KS062 MU#L1 Cl/K
Cl/K
.01
.008
.006
.004
.002
0
0.0
0.2
0.4
0.6
0.8
1.0
Fraction of 39Ar Released

18KS116

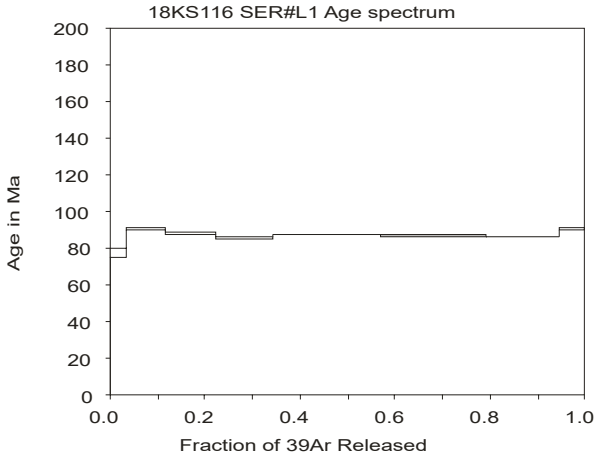
18KS116 SER#L1 Age spectrum
Age in Ma
200
180
160
140
120
100
80
60
40
20
0
0.0
0.2
0.4
0.6
0.8
1.0
Fraction of 39Ar Released

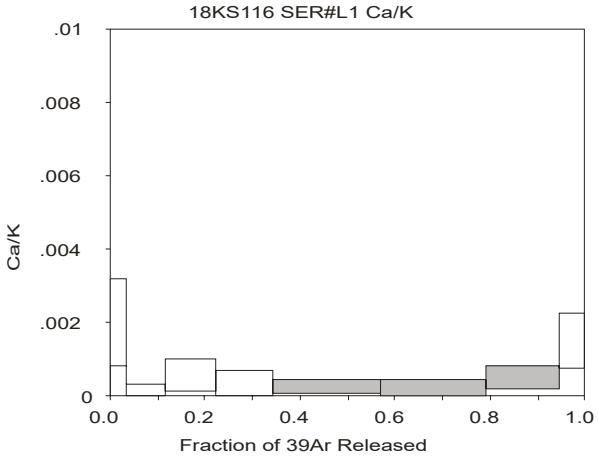
18KS116 SER#L1 Ca/K
Ca/K
.01
.008
.006
.004
.002
0
0.0
0.2
0.4
0.6
0.8
1.0
Fraction of 39Ar Released

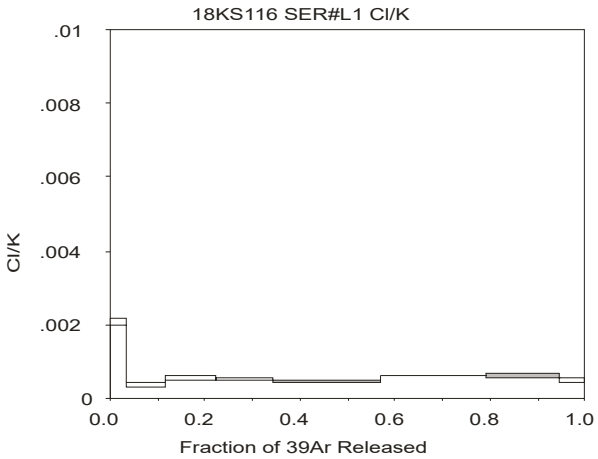
18KS116 SER#L1 Cl/K
Cl/K
.01
.008
.006
.004
.002
0
0.0
0.2
0.4
0.6
0.8
1.0
Fraction of 39Ar Released

18KS131

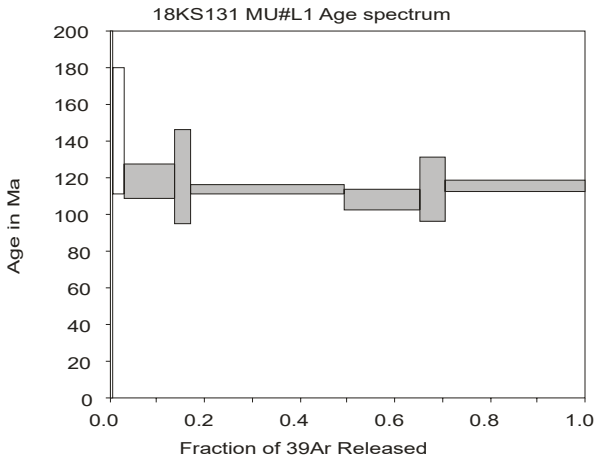
18KS131 MU#L1 Age spectrum
Age in Ma
Fraction of 39Ar Released

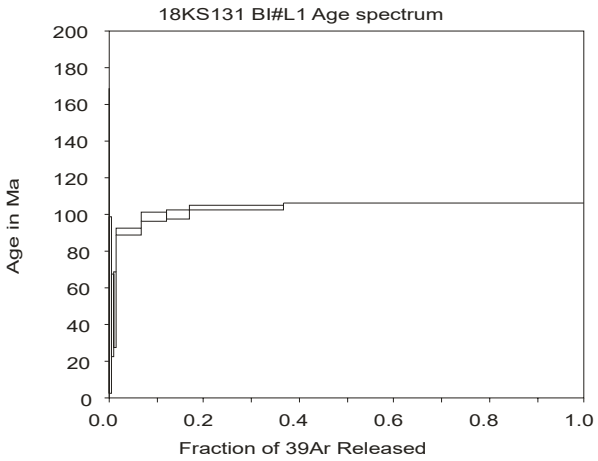
18KS131 BI#L1 Age spectrum
Age in Ma
Fraction of 39Ar Released

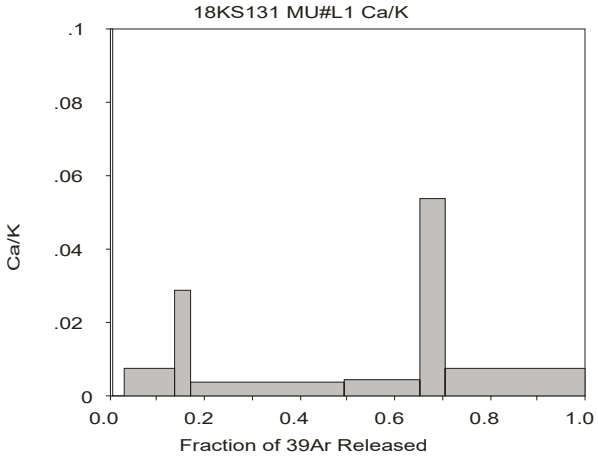
18KS131 MU#L1 Ca/K
Ca/K
Fraction of 39Ar Released

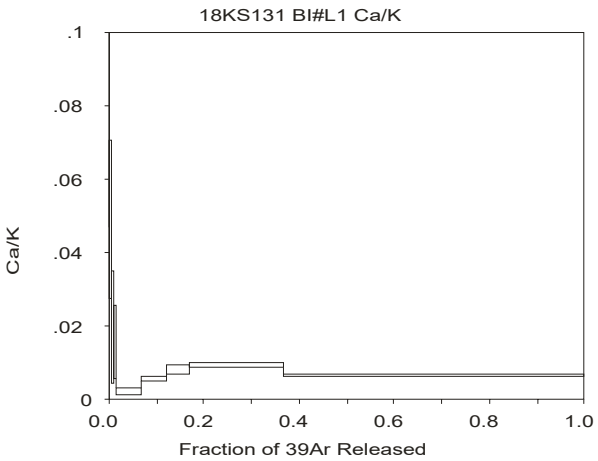
18KS131 BI#L1 Ca/K
Ca/K
Fraction of 39Ar Released

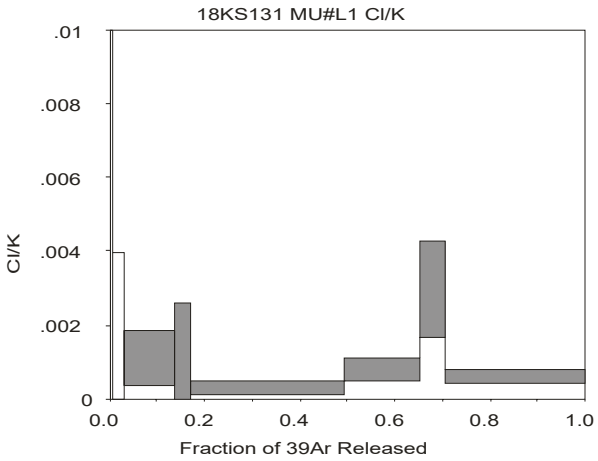
18KS131 MU#L1 Cl/K
Cl/K
Fraction of 39Ar Released

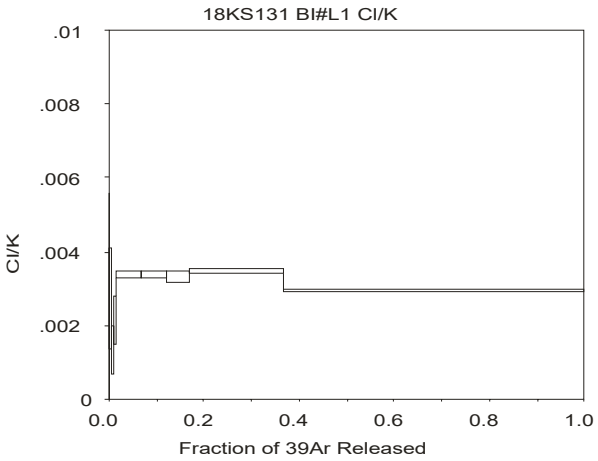
18KS131 BI#L1 Cl/K
Cl/K
Fraction of 39Ar Released

18KS133

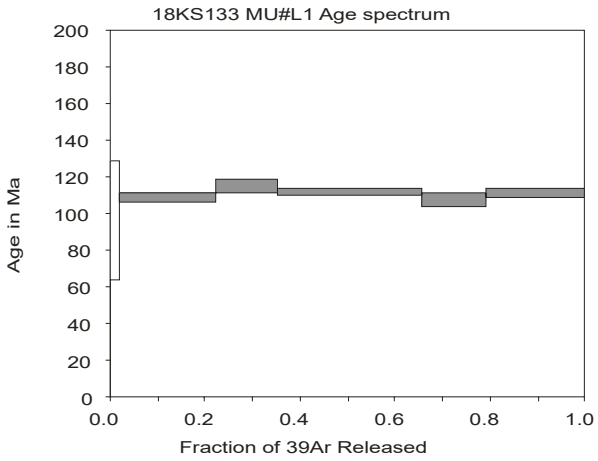
18KS133 MU#L1 Age spectrum
Age in Ma
200
180
160
140
120
100
80
60
40
20
0
0.0
0.2
0.4
0.6
0.8
1.0
Fraction of 39Ar Released

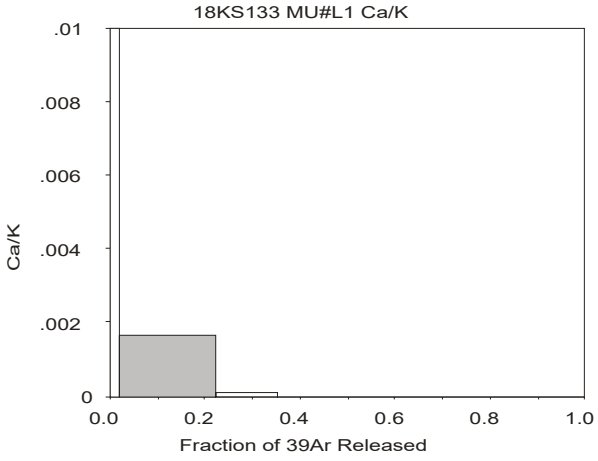
18KS133 MU#L1 Ca/K
Ca/K
.01
.008
.006
.004
.002
0
0.0
0.2
0.4
0.6
0.8
1.0
Fraction of 39Ar Released

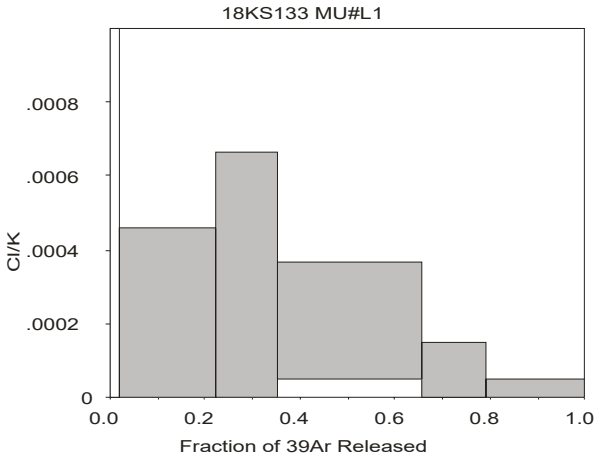
18KS133 MU#L1
Cl/K
.0008
.0006
.0004
.0002
0
0.0
0.2
0.4
0.6
0.8
1.0
Fraction of 39Ar Released

18KS199

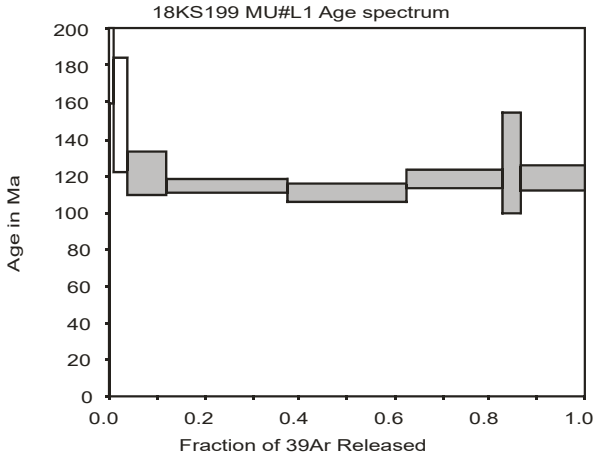
18KS199 MU#L1 Age spectrum
Age in Ma
Fraction of 39Ar Released

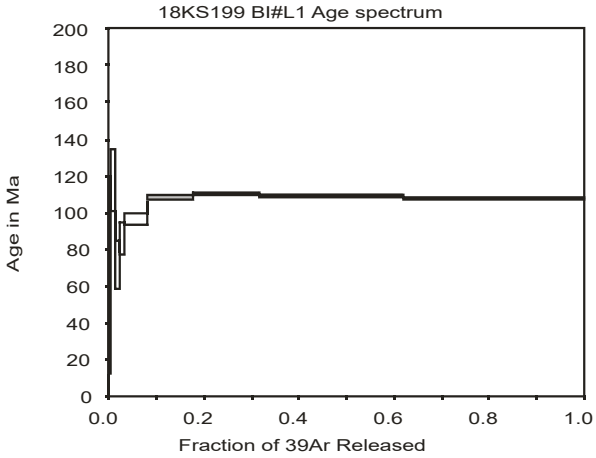
18KS199 BI#L1 Age spectrum
Age in Ma
Fraction of 39Ar Released

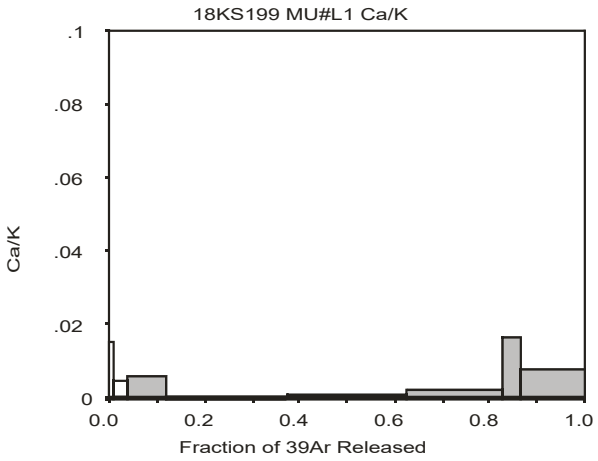
18KS199 MU#L1 Ca/K
Ca/K
Fraction of 39Ar Released

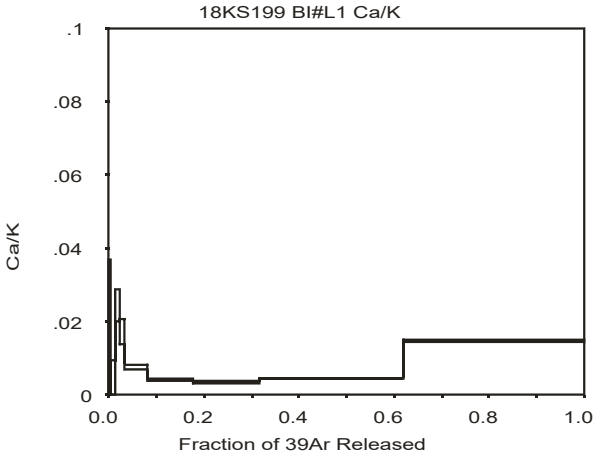
18KS199 BI#L1 Ca/K
Ca/K
Fraction of 39Ar Released

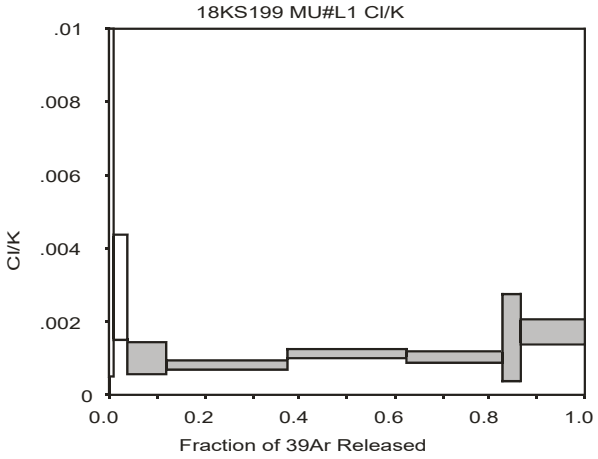
18KS199 MU#L1 Cl/K
Cl/K
Fraction of 39Ar Released

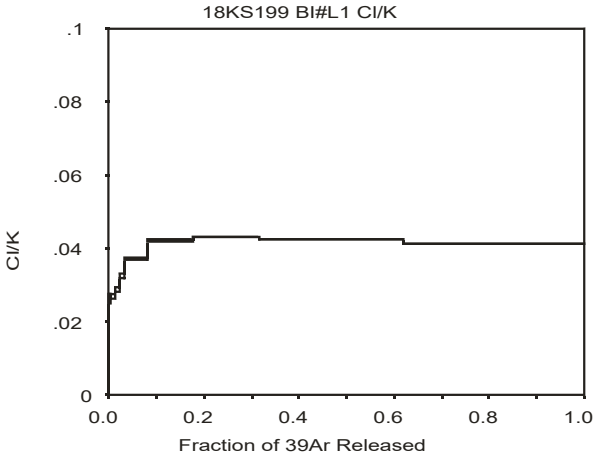
18KS199 BI#L1 Cl/K
Cl/K
Fraction of 39Ar Released

18KS208

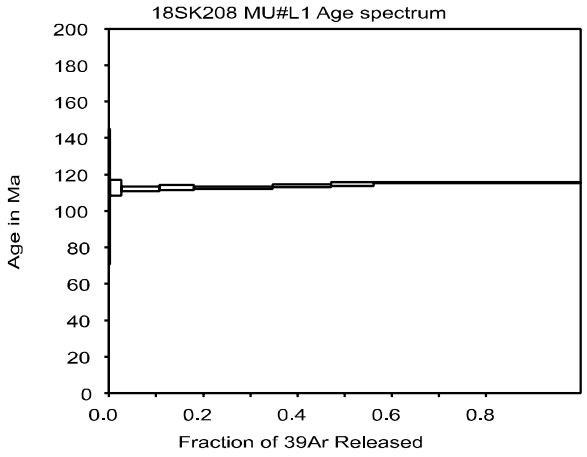
18SK208 MU#L1 Age spectrum
Age in Ma
Fraction of 39Ar Released

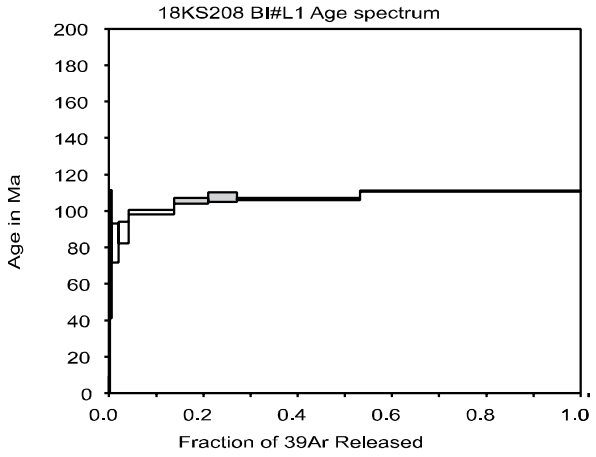
18KS208 BI#L1 Age spectrum
Age in Ma
Fraction of 39Ar Released

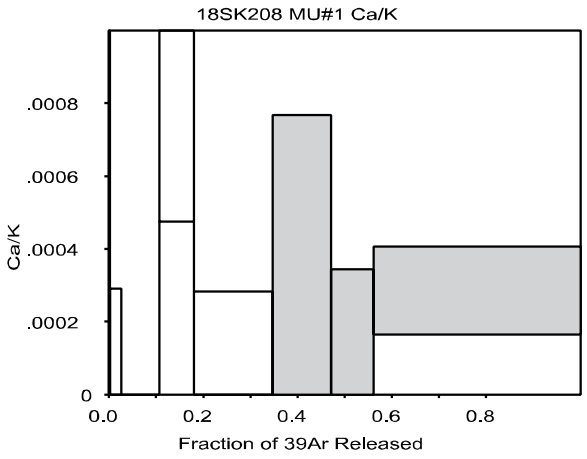
18SK208 MU#1 Ca/K
Ca/K
Fraction of 39Ar Released

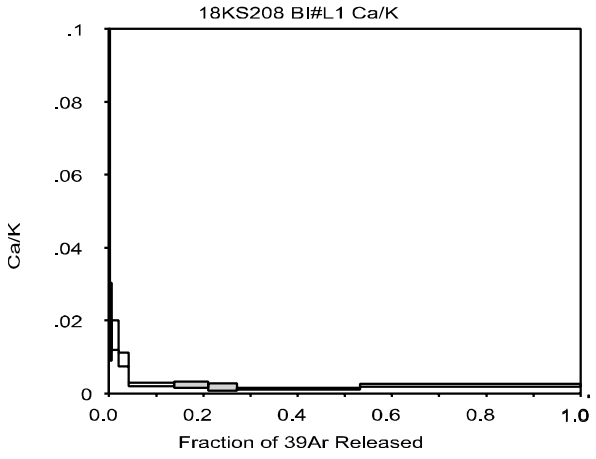
18KS208 BI#L1 Ca/K
Ca/K
Fraction of 39Ar Released

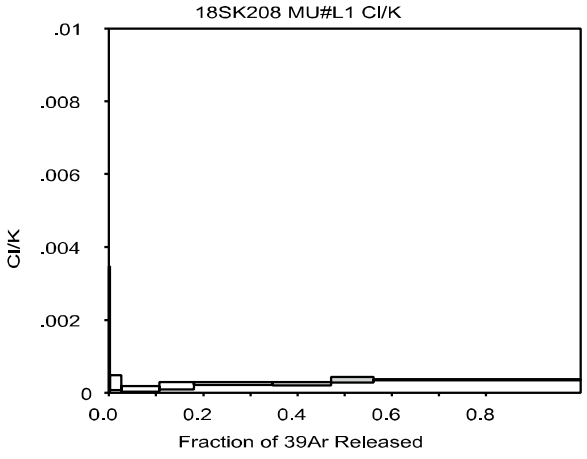
18SK208 MU#L1 Cl/K
Cl/K
Fraction of 39Ar Released

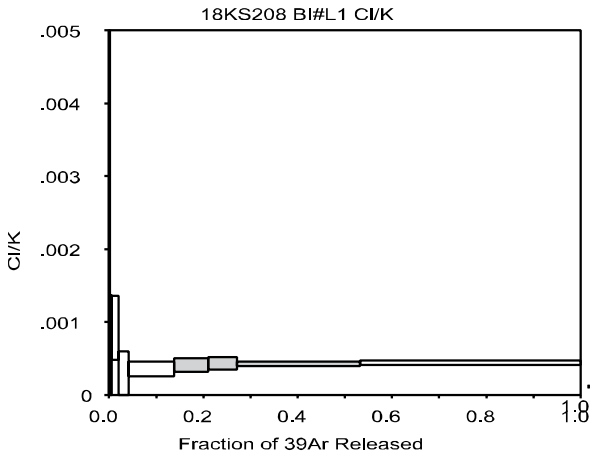
18KS208 BI#L1 Cl/K
Cl/K
Fraction of 39Ar Released

18MBW399

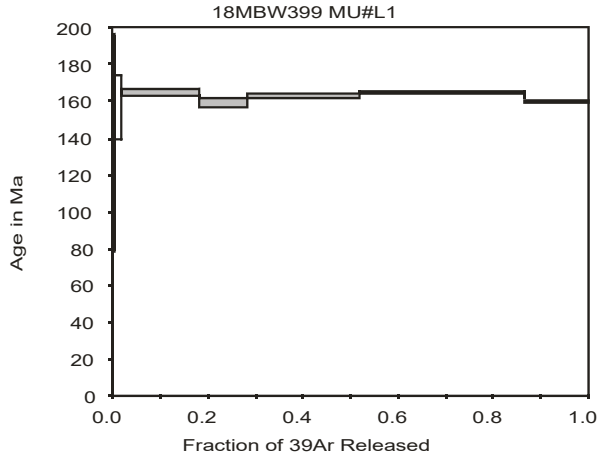
18MBW399 MU#L1
Age in Ma
200
180
160
140
120
100
80
60
40
20
0
0.0
0.2
0.4
0.6
0.8
1.0
Fraction of 39Ar Released

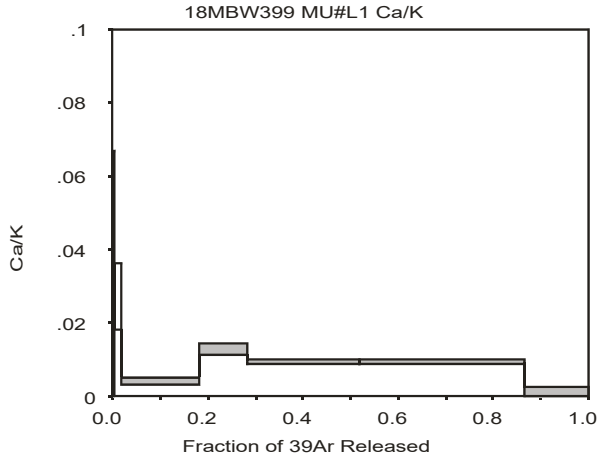
18MBW399 MU#L1 Ca/K
Ca/K
.1
.08
.06
.04
.02
0
0.0
0.2
0.4
0.6
0.8
1.0
Fraction of 39Ar Released

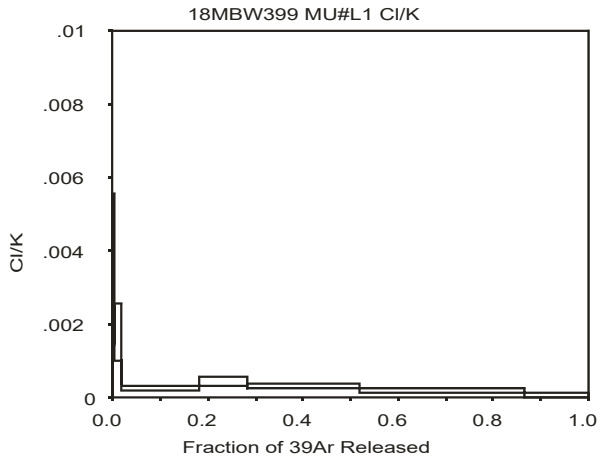
18MBW399 MU#L1 Cl/K
Cl/K
.01
.008
.006
.004
.002
0
0.0
0.2
0.4
0.6
0.8
1.0
Fraction of 39Ar Released

18MLW126

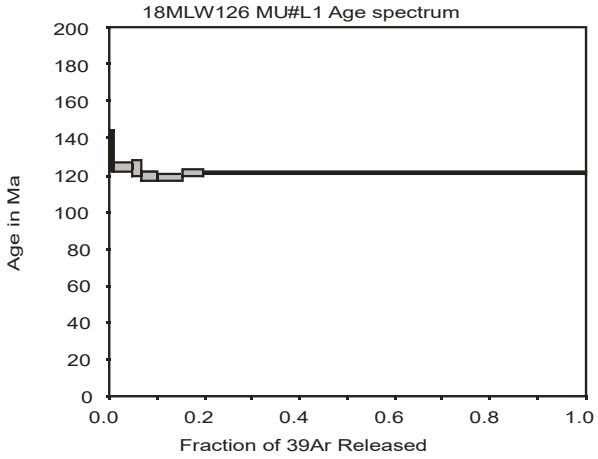
18MLW126 MU#L1 Age spectrum
Age in Ma
Fraction of 39Ar Released

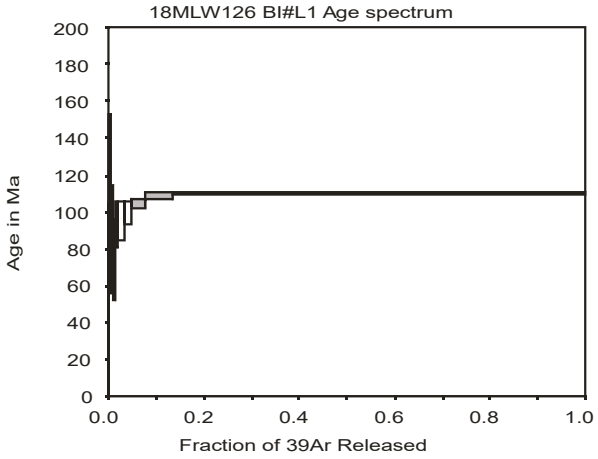
18MLW126 BI#L1 Age spectrum
Age in Ma
Fraction of 39Ar Released

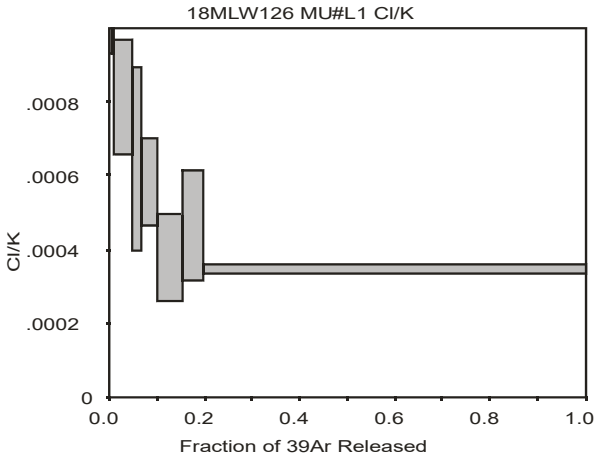
18MLW126 MU#L1 Cl/K
Cl/K
Fraction of 39Ar Released

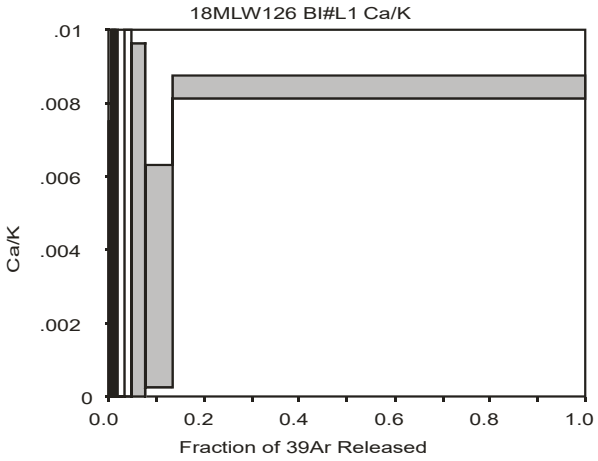
18MLW126 BI#L1 Ca/K
Ca/K
Fraction of 39Ar Released

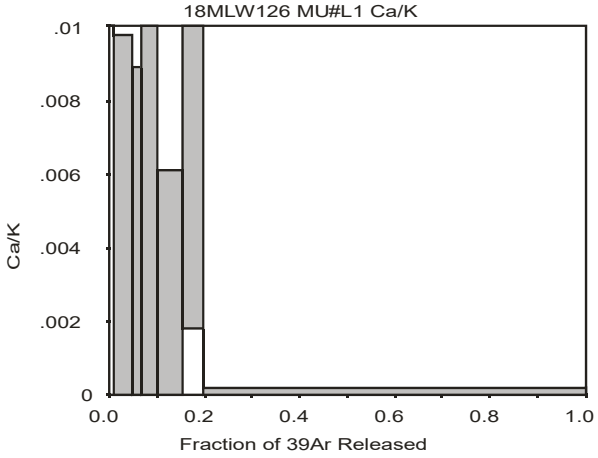
18MLW126 MU#L1 Ca/K
Ca/K
Fraction of 39Ar Released

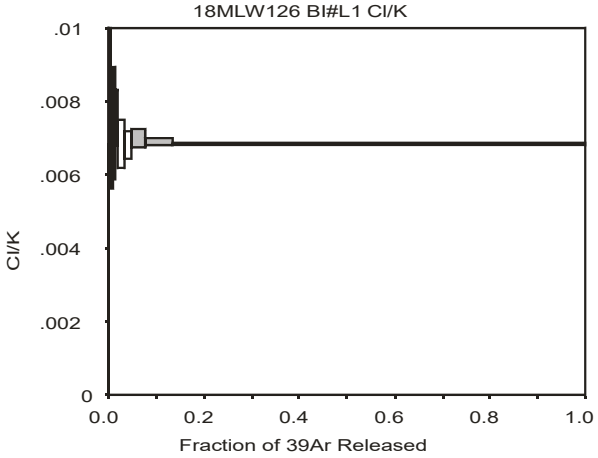
18MLW126 BI#L1 Cl/K
Cl/K
Fraction of 39Ar Released

18MLW132

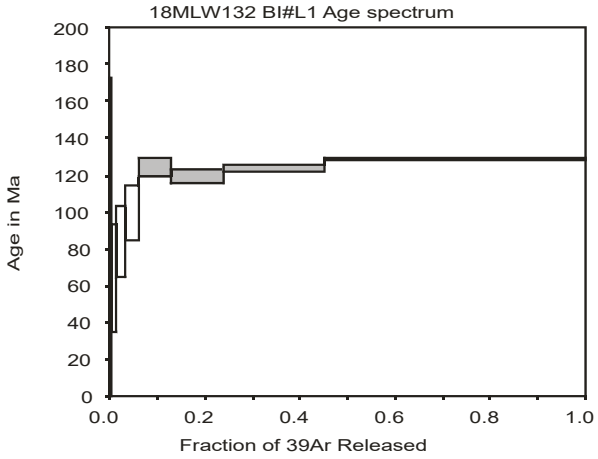
18MLW132 BI#L1 Age spectrum
Age in Ma
200
180
160
140
120
100
80
60
40
20
0
0.0
0.2
0.4
0.6
0.8
1.0
Fraction of 39Ar Released

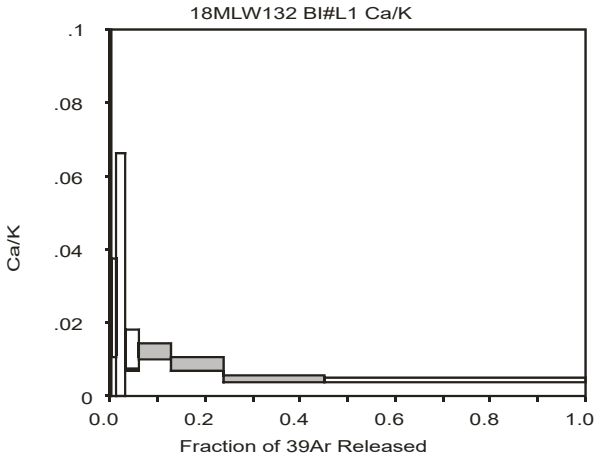
18MLW132 BI#L1 Ca/K
Ca/K
.1
.08
.06
.04
.02
0
0.0
0.2
0.4
0.6
0.8
1.0
Fraction of 39Ar Released

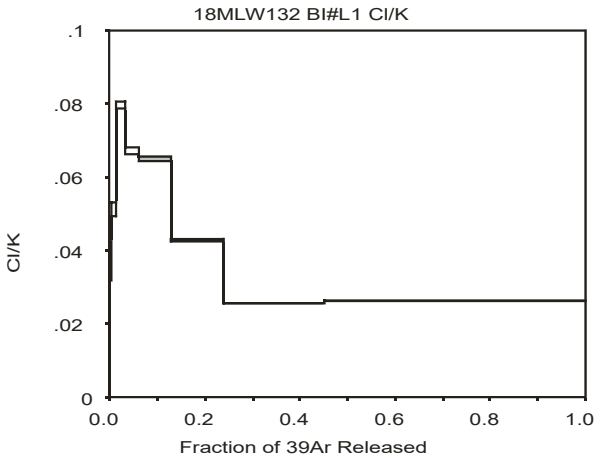
18MLW132 BI#L1 Cl/K
Cl/K
.1
.08
.06
.04
.02
0
0.0
0.2
0.4
0.6
0.8
1.0
Fraction of 39Ar Released

18RN122

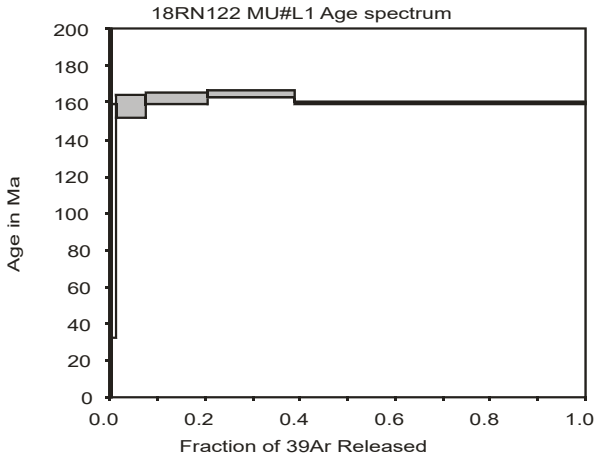
18RN122 MU#L1 Age spectrum
Age in Ma
200
180
160
140
120
100
80
60
40
20
0
0.0
0.2
0.4
0.6
0.8
1.0
Fraction of 39Ar Released

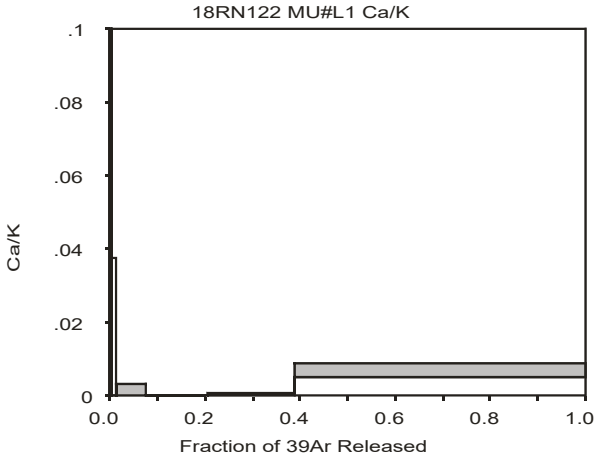
18RN122 MU#L1 Ca/K
Ca/K
.1
.08
.06
.04
.02
0
0.0
0.2
0.4
0.6
0.8
1.0
Fraction of 39Ar Released

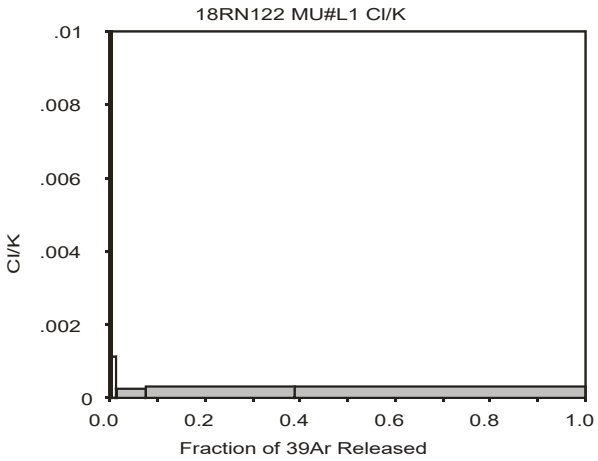
18RN122 MU#L1 Cl/K
Cl/K
.01
.008
.006
.004
.002
0
0.0
0.2
0.4
0.6
0.8
1.0
Fraction of 39Ar Released

18RN259

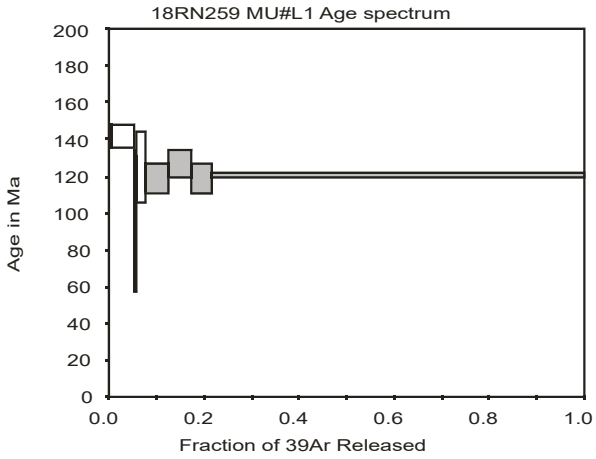
18RN259 MU#L1 Age spectrum
Age in Ma
Fraction of 39Ar Released

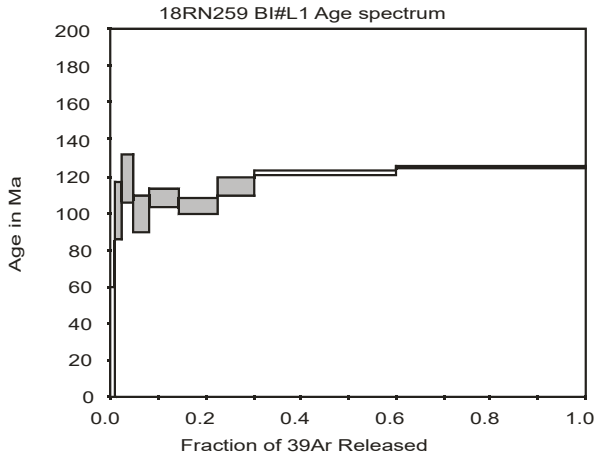
18RN259 BI#L1 Age spectrum
Age in Ma
Fraction of 39Ar Released

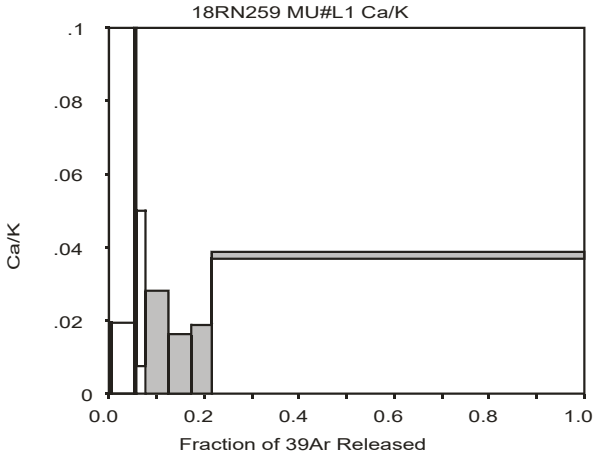
18RN259 MU#L1 Ca/K
Ca/K
Fraction of 39Ar Released

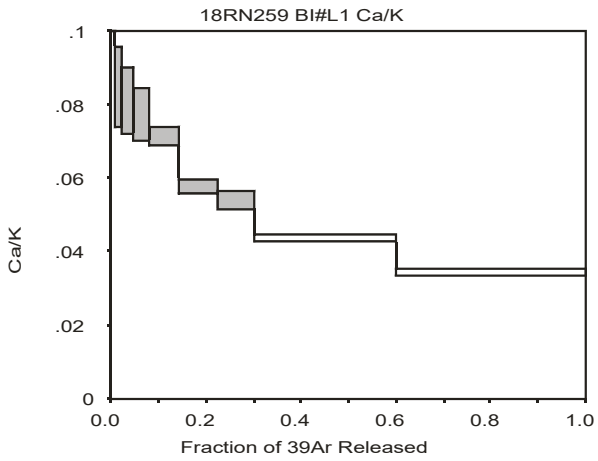
18RN259 BI#L1 Ca/K
Ca/K
Fraction of 39Ar Released

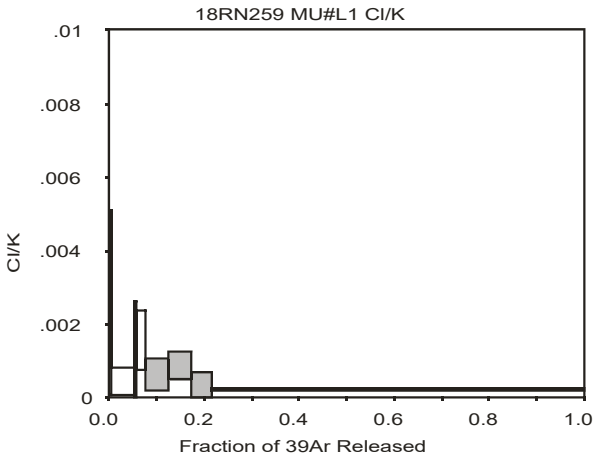
18RN259 MU#L1 Cl/K
Cl/K
Fraction of 39Ar Released

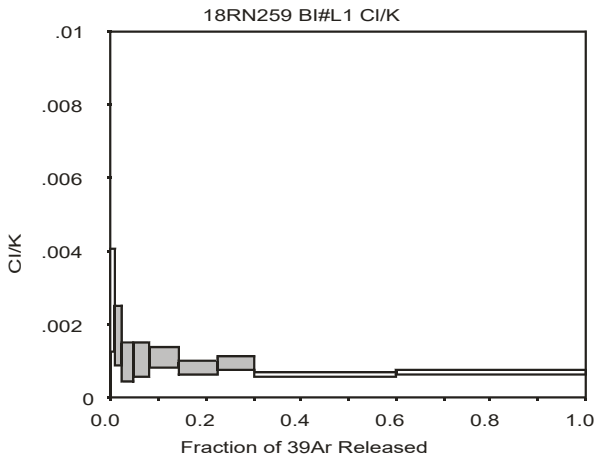
18RN259 BI#L1 Cl/K
Cl/K
Fraction of 39Ar Released

18RN358

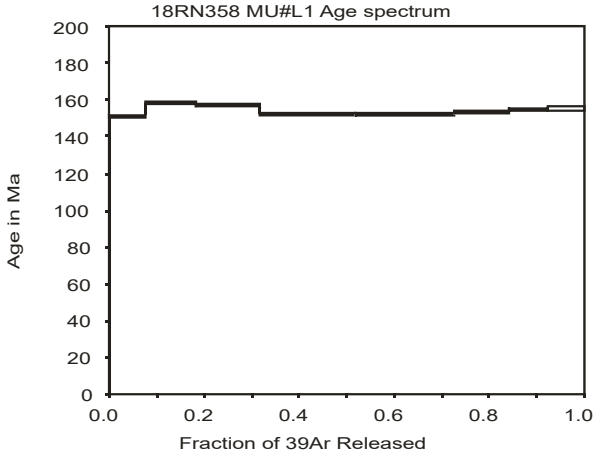
18RN358 MU#L1 Age spectrum
Age in Ma
Fraction of 39Ar Released

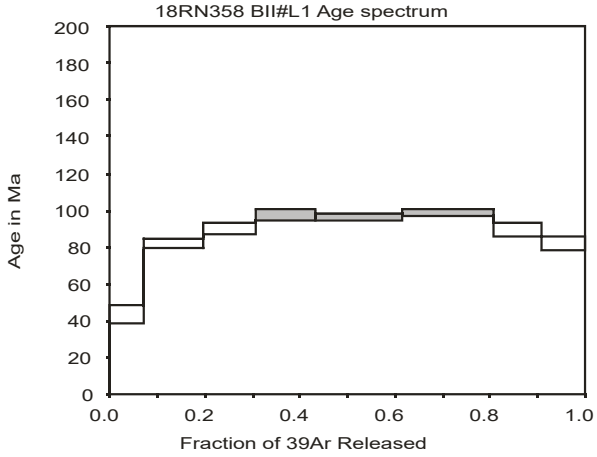
18RN358 BII#L1 Age spectrum
Age in Ma
Fraction of 39Ar Released

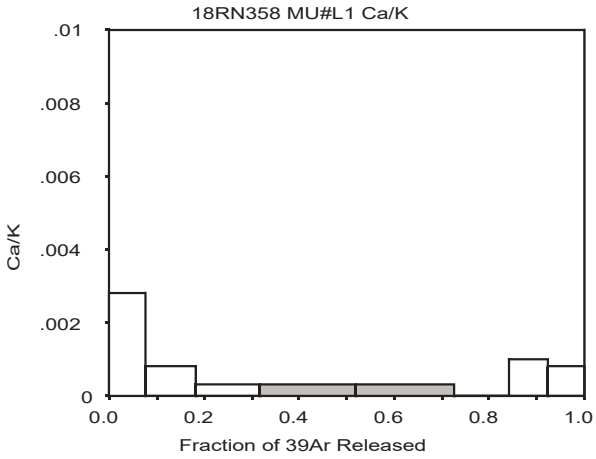
18RN358 MU#L1 Ca/K
Ca/K
Fraction of 39Ar Released

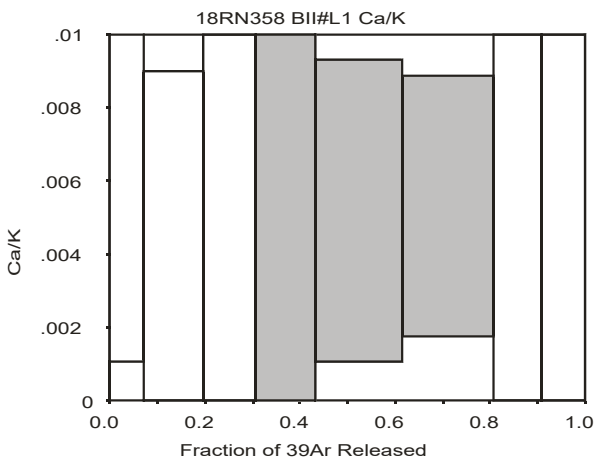
18RN358 BII#L1 Ca/K
Ca/K
Fraction of 39Ar Released

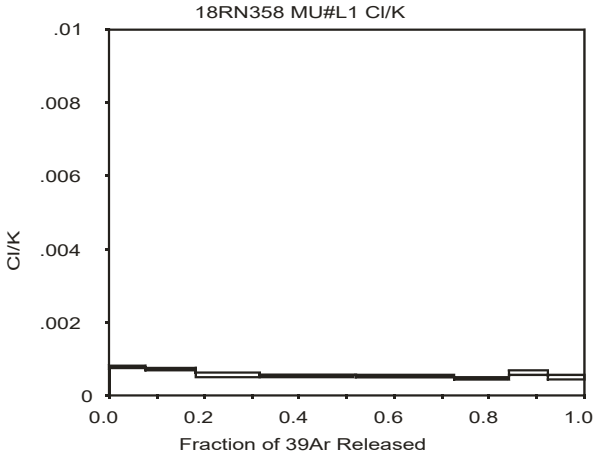
18RN358 MU#L1 Cl/K
Cl/K
Fraction of 39Ar Released

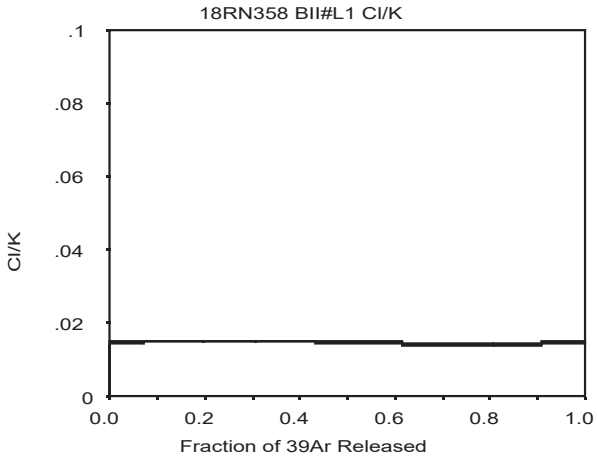
18RN358 BII#L1 Cl/K
Cl/K
Fraction of 39Ar Released

18TJN068

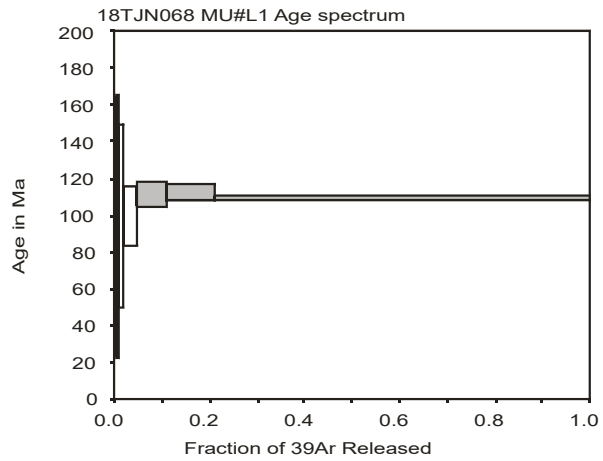
18TJN068 MU#L1 Age spectrum
Age in Ma
Fraction of 39Ar Released

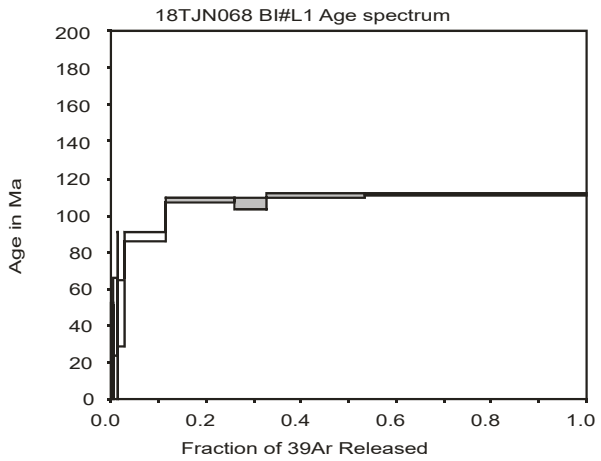
18TJN068 BI#L1 Age spectrum
Age in Ma
Fraction of 39Ar Released

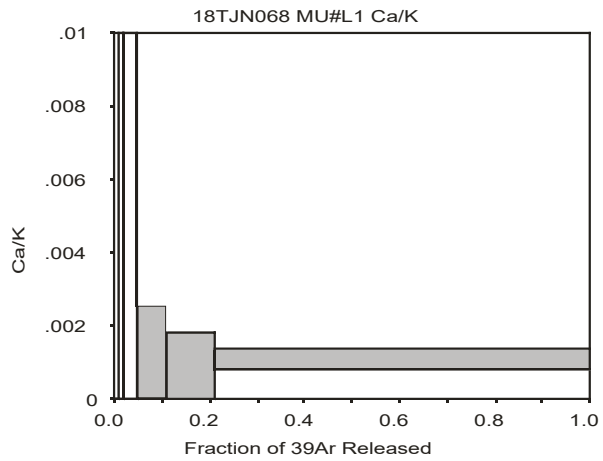
18TJN068 MU#L1 Ca/K
Ca/K
Fraction of 39Ar Released

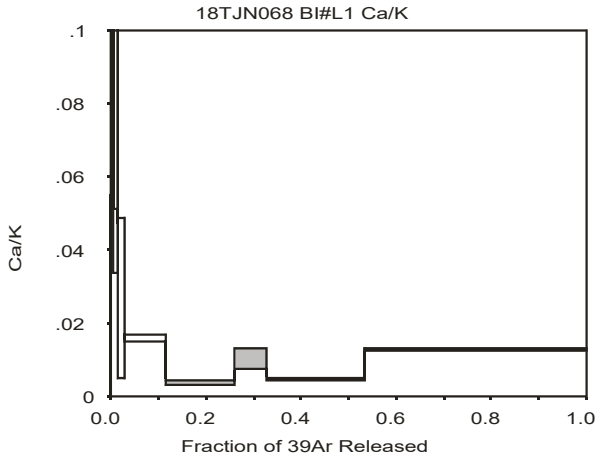
18TJN068 BI#L1 Ca/K
Ca/K
Fraction of 39Ar Released

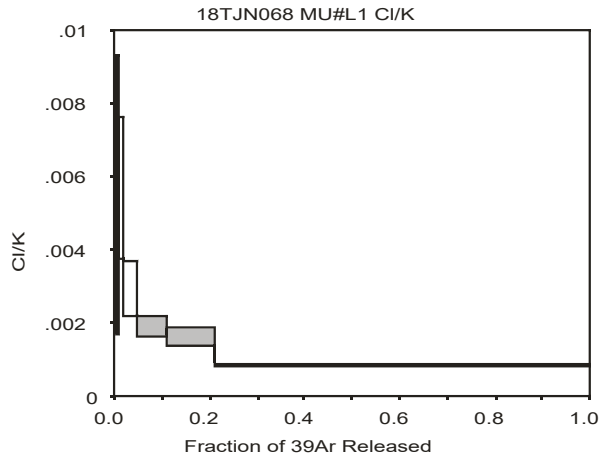
18TJN068 MU#L1 Cl/K
Cl/K
Fraction of 39Ar Released

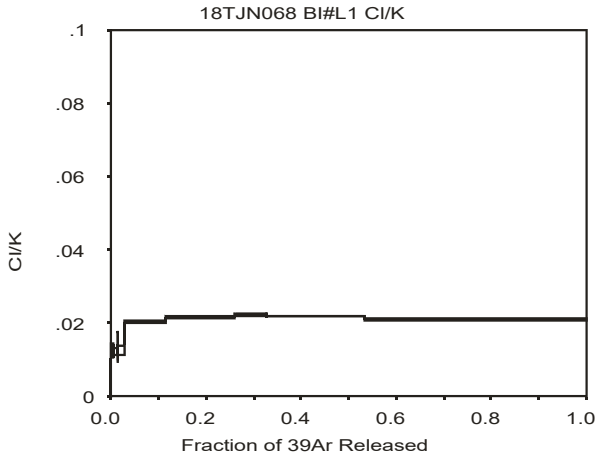
18TJN068 BI#L1 Cl/K
Cl/K
Fraction of 39Ar Released